



Universiti Malaysia  
**KELANTAN**

**INVESTIGATE MICROWAVE ABSORPTION ON  
FORMULATED SiC/Al<sub>2</sub>O<sub>3</sub> COMPOSITE POROUS  
SUSCEPTOR**

by

**SITI ZURAINA BINTI NAWAWI**

A report submitted in fulfillment of the requirements for the degree of  
Bachelor of Applied Science (Materials Technology) with Honours

---

**FACULTY OF EARTH SCIENCE  
UNIVERSITI MALAYSIA KELANTAN**

---

2017

## DECLARATION

I hereby declare that I have conducted, completed the research work and written the dissertation entitled “Investigate Microwave Absorption on Formulated SiC/Al<sub>2</sub>O<sub>3</sub> Composite Porous Susceptor”. I also declare that it has not been previously submitted for the award of any degree or diploma or other similar title of this for any other examining body of university

Signature : \_\_\_\_\_

Name : Siti Zuraina binti Nawawi

Date : 12/01/2017

UNIVERSITI  
MALAYSIA  
KELANTAN

## ACKNOWLEDGEMENT

First and foremost, I would like to thank Earth Science Faculty, Universiti Malaysia Kelantan (UMK), Dean of faculty in providing me opportunity to complete this final year research project in an appropriate and good environment.

Next, I would like to express my deepest gratitude to my helpful and patient supervisor and co-supervisor, Dr. Muhammad Azwadi bin Sulaiman and Dr. Julie Juliewatty binti Mohamed for the support, guidance, encouragement and time throughout the two semester to complete this final year project.

I would like to show my appreciation to the technicians, academic and administrative staffs which have helped me throughout my research here. All their responsibility and useful advice which aid me to complete this final year project.

Last but not least, I would like to thank my fellow friends, especially Nurul Zaffiqah binti Zamzuri and Nurul Ainon binti Bakar for invaluable sharing and constructive suggestion also guidance to complete this research

UNIVERSITI  
MALAYSIA  
KELANTAN

## INVESTIGATE MICROWAVE ABSORPTION ON FORMULATED SiC/Al<sub>2</sub>O<sub>3</sub> COMPOSITE POROUS SUSCEPTOR

### ABSTRACT

Electricity is the main cost of production in the manufacturing industry. Thus, the best way is by optimum the energy consumption from the sources, use as much as it can and shorter the time for the process which consume energy. Understand this needs, susceptor usage in a microwave is the best alternative to absorb the energy sources and convert the energy in less time. However, the commercially susceptor which is SiC susceptor has low electromagnetic absorption which consume more energy and high cost to produce since it is pure Silicon Carbide and need high sintering temperature. In this studies, high electromagnetic absorption of SiC/Al<sub>2</sub>O<sub>3</sub> composite susceptor produced which enhanced electromagnetic absorption, lower the sintering temperature that cut the cost of production so it can be use in domestic application. The studies use different compositions of Alumina and Silicon Carbide as fillers which are (10, 20, 30, 40 and 50 wt% Al<sub>2</sub>O<sub>3</sub>). The raw material, mixture and the sintered composite were characterize in term of phase characterization, microstructure, electromagnetic absorption and density and porosity to determine the best composition to fabricate the SiC/Al<sub>2</sub>O<sub>3</sub> composite susceptor. Result shows 50 wt% of Alumina be able to reach 556°C within 12 minutes, and in term of microstructure, XRD also density and porosity, it is ideal among the five composition. This ideal ratio uses for the production of porous susceptor using 5 different pore size of sponge. The porous structure able to absorb more energy from microwave rays. The sponge replication method uses and this studies find the best pore size of sponge is 191.9523 μm. This size reach up to 591°C.

UNIVERSITI  
MALAYSIA  
KELANTAN

# MENYELIDIK GELOMBANG MIKRO TERHADAP SUSCEPTOR BERFORMULA SiC/Al<sub>2</sub>O<sub>3</sub> KOMPOSIT

## ABSTRAK

Elektrik merupakan keperluan utama untuk pengeluaran dalam industri pembuatan. Oleh itu, cara yang terbaik adalah dengan optimum penggunaan tenaga daripada sumber-sumber, gunakan sebagai sebaik mungkin kerana ia boleh dan kurang masa untuk proses yang menggunakan tenaga. Memahami ini perlu, penggunaan susceptor di dalam gelombang mikro adalah alternatif terbaik untuk menyerap sumber tenaga dan menukarkan tenaga dalam masa singkat. Walau bagaimanapun, susceptor secara komersial yang SiC susceptor mempunyai penyerapan elektromagnet rendah yang mengambil lebih banyak tenaga dan kos yang tinggi untuk menghasilkan kerana ia adalah silikon karbida tulen dan memerlukan suhu pembakaran tinggi. Dalam kajian ini, penyerapan elektromagnet tinggi SiC/Al<sub>2</sub>O<sub>3</sub> susceptor komposit dihasilkan untuk meningkatkan penyerapan elektromagnet, menurunkan suhu pensinteran yang mengurangkan kos pengeluaran supaya ia boleh digunakan dalam aplikasi domestik. Kajian menggunakan komposisi yang berbeza daripada Alumina dan silikon karbida sebagai pengisi iaitu (10, 20, 30, 40 dan 50 wt.% Al<sub>2</sub>O<sub>3</sub>). Bahan mentah, campuran dan komposit tersinter telah mencirikan dari segi pencirian fasa, mikrostruktur, penyerapan elektromagnet dan ketumpatan dan keliangan untuk menentukan komposisi yang terbaik untuk mereka-reka yang susceptor komposit SiC/Al<sub>2</sub>O<sub>3</sub>. Keputusan menunjukkan 50% berat Alumina dapat mencapai 556°C dalam masa 12 minit, dan dalam jangka mikrostruktur, XRD juga ketumpatan dan keliangan, ia adalah sesuai antara lima komposisi. Ini nisbah ideal digunakan untuk pengeluaran susceptor berliang menggunakan 5 span saiz liang yang berbeza. Struktur berliang mampu menyerap lebih banyak tenaga daripada sinaran gelombang mikro. Kaedah span replikasi digunakan dan kajian ini mendapati saiz liang span yang terbaik adalah 191.9523 mikron meter. Saiz ini mencapai 591°C.

UNIVERSITI  
MALAYSIA  
KELANTAN

## Table of Contents

DECLARATION	i
ACKNOWLEDGEMENT	ii
ABSTRACT	iii
ABSTRAK	iv
LIST OF TABLES	vii
LIST OF FIGURES	viii
LIST OF ABBREVIATIONS	ix
LIST OF SYMBOL	x
CHAPTER 1:INTRODUCTION	1
1.1 Background of Study	1
1.2 Problem Statement	4
1.3 Objective	5
1.4 Expected Outcome	5
CHAPTER 2:LITERATURE REVIEW	6
2.1 Materials Background	6
2.2 Ceramic Composite Susceptor	6
2.3 Properties of Ceramic and Composite Ceramic	8
2.3.1 Phase Characterization	10
2.3.2 Microstructure	12
2.3.3 Electromagnetic Absorption	12
2.3.4 Density and Porosity	13
2.3.5 Dielectric Loss	13
CHAPTER 3:MATERIALS AND METHODS	15
3.1 Experimental Process	15
3.2 Raw Materials Characterizations	15
3.3 Processing Methods	18
3.4 Material Characterizations	19
3.4.1 Phase Analysis (XRD)	19
3.4.2 Microstructure (Optical Microscope)	20
3.4.3 Density and Porosity Measurement	20
3.4.4 Electromagnetic	20
3.4.5 Dielectric Properties	21
CHAPTER 4:RESULT AND DISCUSSION	22
4.1 Introduction	22

4.2	Raw Materials	23
4.3	Mixing Process	26
4.4	Composite Product	28
4.4.1	Characterization of Composite Product	29
4.5	Porous Composite Product	36
4.5.1	Electromagnetic Absorption	36
CHAPTER 5: CONCLUSION AND RECOMMENDATION		38
5.1	Conclusion	38
5.2	Recommendation	39
REFERENCES		40
APPENDIX		43

## LIST OF TABLES

No.		Page
3.1	Composition of SiC/Al <sub>2</sub> O <sub>3</sub> Composite	18
4.1	The microstructure of sintered composite	32





## LIST OF FIGURES

No.		Page
2.1	Structure of Alumina in which half of the Al ions are occupy tetrahedral sites (Shirai et al., 2009)	13
2.2	(a) Corundum structure of $\alpha$ -Al <sub>2</sub> O <sub>3</sub> , (b) Top view of the corundum structure, and (c) Octahedral structure of $\alpha$ -Al <sub>2</sub> O <sub>3</sub>	13
2.3	Tetrahedral building block of SiC crystal. (a) Four carbon atoms bonded to one silicon atom (b) Four silicon atoms bonded to one carbon atom	14
3.1	The flowchart of research in this study	17
4.1	The Silicon Carbide	19
4.2	The Aluminium Oxide	19
4.3	XRD Pattern of Al <sub>2</sub> O <sub>3</sub> (COD 9009671)	22
4.4	XRD Pattern of SiC (COD 1011053)	23
4.5	Sponge pore size	24
4.6	The composite before sintering process	25
4.7	Figure 4.7: XRD pattern of SiC/Al <sub>2</sub> O <sub>3</sub> composite after mixing process, (a) 50 wt% SiC/Al <sub>2</sub> O <sub>3</sub> , (b) 40 wt% SiC/Al <sub>2</sub> O <sub>3</sub> , (c) 30 wt% SiC/Al <sub>2</sub> O <sub>3</sub> , (d) 20 wt% SiC/Al <sub>2</sub> O <sub>3</sub> , (e) 10 wt% SiC/Al <sub>2</sub> O <sub>3</sub>	26
4.8	The composite after sintering process	27
4.9	XRD pattern of SiC/Al <sub>2</sub> O <sub>3</sub> composite sintering process, (a) 50 wt% SiC/Al <sub>2</sub> O <sub>3</sub> , (b) 40 wt% SiC/Al <sub>2</sub> O <sub>3</sub> , (c) 30 wt% SiC/Al <sub>2</sub> O <sub>3</sub> , (d) 20 wt% SiC/Al <sub>2</sub> O <sub>3</sub> , (e) 10 wt% SiC/Al <sub>2</sub> O <sub>3</sub>	28
4.10	The density of composite with different composition	30
4.11	The porosity of composite with different composition	30
4.12	The electromagnetic absorption with time of composite	31
4.13	The electromagnetic absorption with time of porous composite using different sponge pore size	34

## LIST OF ABBREVIATIONS

SiC	Silicon Carbide
Al <sub>2</sub> O <sub>3</sub>	Alumina
IR	Infrared
XRD	X-ray Diffraction
SEM	Scanning Electron Microscopy
EM	Electromagnetic
EDX	Energy-dispersive X-ray Spectroscopy
ASTM	American Standard Testing Machine

UNIVERSITI  
MALAYSIA  
KELANTAN

## LIST OF SYMBOL

%	Percentage
°C	Degree Celsius
$\rho$	Density
h	Hour
cm	Centimeter
wt.	Weight
a.u	Arbitrary Unit
g	Gram
$\mu$	Micro
m	meter



UNIVERSITI  
MALAYSIA  
KELANTAN

# CHAPTER 1

## INTRODUCTION

### 1.1 Background of Study

Composite is combination of two or more materials to form a new material system with enhanced material properties. Composite are made up of matrix and reinforcement. The composite can be metal matrix composite, polymer matrix composite or ceramic matrix composite. Composite is one of the solution to improve mechanical properties, fatigue endurance, toughness, versatility and tailoring also cut the cost. The matrix added to act as binder, provide rigidity, increase surface quality, protection of wear and corrosion. The reinforcement in form of fibers, sheets, or particles provide structural properties and modification of electrical conductivity or insulation (Naga, 2014). The composite suitable to various application such as automotive, aerospace, marine, biomedical purpose and electronic parts. Making the composite overcome the weakness of original material so avoid the failure of the material system in the future.

Metal matrix composite be used at various application such as aerospace (Badiger *et al.*, 2015), which involve high temperature exposure. Metal use in composite are aluminium, magnesium, titanium, and copper which are alloy that use in high operating temperature, nonflammability, and greater resistance to degradation by organic fluids environment (Callister, 2010). Composite of metals are synthesized to improve high strength (Srivastava *et al.*, 2016), less brittle (Kurşun *et al.*, 2016) and

be able to plastically deform (Leong *et al.*, 2015) to the heat and pressure impact. The present research deals with the synthesis of some Al–Gr composites, the effect of three different metals as Cu, Ni and Ag on the graphite and Al/MeGr interphase and the evaluation of process conditions which are type of additive, their concentration and milling intensity on the characteristics of the processed powders and their mechanical performance (Duarte *et al.*, 2015). This could overcome the disadvantage of metal is high melting point that increase the cost of production.

Polymer matrix composites are used in various industrial production field can be thermoset or thermoplastic. Thermoset have extensive cross-linking formed by covalent bonds which prevent chains moving relative to each other so it have rigid shape (Deng *et al.*, 2015). Meanwhile thermoplastic has weak attractive forces between chains that can be broken by warming and it can change it shape when remoulded. Through chemical synthesis, the polymer can be utilized according to the work ability (Duan *et al.*, 2016). The disadvantages of polymer are unstable in term at thermal and mechanical properties. Polymer also have low elasticity, low melting temperature and mechanical stability, low resistance to oxidation and UV radiation. Producing composite of polymer, the reinforcement overcome those weakness of polymer properties.

Ceramic matrix composite (CMC) are used in the application of biomedical (Chen, *et al.*, 2014), gas turbine (Naga, 2014; Osada *et al.*, 2014), cutting tools (Zhao, 2014), automotive (Yin & Stoll, 2014) and electronic (Mu *et al.*, 2015). The ceramic use to be composite is oxide ceramic commonly  $\text{TiO}_2$ ,  $\text{Al}_2\text{O}_3$ ,  $\text{CuO}$  and non-oxide ceramic such as  $\text{SiC}$ . These original ceramic is brittle (Genua *et al.*, 2011) and low toughness (Xia *et al.*, 2014). Hence, reinforcement and matrix used increases the resistance and crack density (Osada *et al.*, 2014) as original ceramic is. It also can be

modified to provide corrosion resistance, thermal shock resistance, modulus, toughness and strength (Xia *et al.*, 2014). The CMC generally fabricated into a dense or porous. The dense ceramics can be fabricate by compaction of powder while porous ceramics can be efficiently fabricated using hollow beads, in which hollow spheres are added as pore forming agents into ceramic matrix, and the closed pores are reserved after hollow spheres melt into matrix (Sun *et al.*, 2016)

Alumina ( $\text{Al}_2\text{O}_3$ ) is compound contain inorganic fibers (Cooke, 1991) and has high temperature resistance and high compression modulus value. In electronic application, alumina has high thermal conduction and high electrical insulators. The use of alumina is low cost and effective in conductive application. The particle in spherical shape with microns' particle increase the controllable of its electronic behavior. Alumina is white powder from bauxite ores go through refining process. The purify of alumina grade in commercial market are various and still in the development (Rybakov *et al.*, 2013). Commercial grades of  $\text{Al}_2\text{O}_3$  are often divided into smelter, calcined (milled or unmilled), low soda, reactive, tabular, activated, catalytic, and high purity (Shirai *et al.*, 2009).

Silicon carbide (SiC) was accidentally discovered in 1890 by Edward G. Acheson, an assistant to Thomas Edison, when he was running an experiment on the synthesis of diamonds. Acheson thought the new material was a compound of carbon and alumina present in the clay, leading him to name it carborundum, a name that is still being used on some occasions. Silicon carbide occurs naturally in meteorites, though very rarely and in very small amounts. Being the discoverer of SiC, Acheson was the first to synthesize SiC by passing an electric current through a mixture of clay and carbon. Today, SiC is produced via a solid state reaction between sand (silicon

dioxide) and petroleum coke (carbon) at very high temperatures in an electric arc furnace (Graphite, 2002).

Silicon Carbide (SiC) is a stable material for thermal, mechanical and chemical properties (Carvalho *et al.*, 2008). It has high dielectric loss, high thermal stability at high temperature (Yang *et al.*, 2013). These special properties aid to withstand harsh condition which the stress and thermal are exposed. SiC is one of the ceramic which have been used to make susceptor. SiC susceptor are sintered at high sintering temperature up to 2000°C (Sulaiman *et al.*, 2014) and the high cost of SiC raw materials make it difficult to be manufactured at low cost (Xu *et al.*, 2016).

The understanding of SiC relatively as high temperature ceramics material also shows rapid detection method development with high sensitivity for detecting the variation of contents of components (e.g., carbon, oxygen, and silicon) (Li *et al.*, 2016). The most common forms of SiC include powders, fibers, whiskers, coatings and single crystals. There are several methods to produce SiC depending on the product form desired and its application. Purity of the product imposes certain restrictions on the selection of the method of production (Graphite, 2002)

## 1.2 Problem Statement

In the making of susceptor, SiC had been used as raw material which offer good mechanical properties. The needs of sintering temperature at high up to 2000°C, it makes the cost of production are high and lead to ineffective used of energy. To skip the costly sintering temperature, the SiC powder can be bound together by secondary phase as the binder. In this case of susceptor application, alumina has high potential due to low electromagnetic absorption. By introducing composite SiC with alumina,

the sintering temperature can be decreased to 1300°C so the cost of production can be decreases (Galusek *et al.*, 2014).

The commercial SiC susceptor is solid material that have low total surface area. The composite susceptor of SiC/Al<sub>2</sub>O<sub>3</sub> with high porous structure will increase the total surface area so it capable to increase the energy conversion which aid to effective energy used in firing process.

### 1.3 Objective

The objectives of this research are:

- i. To synthesize SiC/Al<sub>2</sub>O<sub>3</sub> composite at different composition.
- ii. To synthesize various of SiC/Al<sub>2</sub>O<sub>3</sub> composite using slip casting and sponge replication method.
- iii. To optimize electromagnetic absorption of the composite.

### 1.4 Expected Outcome

At the end of this research, the optimize composition of the composite will be identified and can be compared with the previous work. Also, high electromagnetic absorption of SiC/Al<sub>2</sub>O<sub>3</sub> susceptor will be produced which enhanced electromagnetic absorption, lower the sintering temperature that cut the cost of production so it can be use in domestic application.



## CHAPTER 2

### LITERATURE REVIEW

#### 2.1 Materials Background

The research of composite of SiC with other metal systems such as copper, aluminum, tungsten, titanium and hard metals have also been successfully sintered using microwaves (Leong *et al.*, 2015). The varies of the material determine its performance as a matrix in high temperature. In this research, Alumina had been chosen to use as a matrix. The composite of Alumina and Silicon Carbide had been done and the consistency of the result are still experimented as it is still new in this field.

#### 2.2 Ceramic Composite Susceptor

Susceptor is lossy material used in the commercial microwave heating process frequencies between 300 MHz and 300 GHz (Clark *et al.*, 2000). Bhattacharya *et al.*, (2016) stated the susceptor absorb and transfer electromagnetic (EM) via providing heating process with reduced heat losses from the material surface. This proved by Heuguet *et al.*, (2013) that the role of a susceptor is to couple with microwaves, especially at low temperature, to initiate the heating of low coupling materials (low dielectric loss materials).

Heuguet *et al.*, (2013) also view the susceptor heats by itself at low temperature and transmits the heat to the sample by IR radiation and when it reaches certain temperature, the sample starts to heat by itself and its overall heating results from both microwave coupling and IR radiation, emitted by the susceptor. The mechanism of susceptor from Vargas *et al.*, (2016) was started when the susceptor absorb the microwave EM, vibrate the susceptor atom and produce heat. The beneficial of using the susceptor is it can associated with the microwave processing providing rapid and uniform heating, decreased sintering temperatures, improved physical and mechanical properties (Clark *et al.*, 2000) also quicker processing as well as minimal diffusion of dopants during annealing (Wang, 2005).

Firstly, microwave sintering studies focused on ceramic susceptors commercially SiC susceptor (Bhattacharya *et al.*, 2016). It due to the intensity of the electric field within the sample is higher than the one when SiC susceptor is used and high microwave absorption of SiC also can be related with the thermal profile which exhibits an immediate and steady increase of the temperature (Heuguet *et al.*, 2013). From Leong *et al.*, (2015) hybrid microwave sintering, the heating rate can be varied by controlling the amount of SiC susceptor added and the size of SiC particles used. Also reported, a significant reduction of the processing time during the hybrid sintering of the MgO and ZrO<sub>2</sub> doped mullites in the presence of SiC susceptors (Bodhak, 2011).

Research continued find the Alumina ceramic plate with low raw material cost with excellent microwave energy absorption (Mandal *et al.*, 2014). Bind SiC with Alumina to achieve the required temperatures for repairing the lattice damage (Alford *et al.*, 2012) had shown the tendency of it in manage the atom in the composite at the definite temperature. To strengthen the composite, the production of a fine and homogeneous distribution of hardening particles with a very fine particle size used the

solid-state or mechanical milling (MM) route so that final composite produce are at their best depends of their specific characteristics which are particle type, size, morphology, volume fraction and their physical distribution (Duarte *et al.*, 2015). The composite of alumina matrix with SiC improved the energy transfer in the microwave heating. It also invaluable in their ability to be engineered for specific stress, temperature, life, and environmental conditions (Aeronautics, n.d.).

Al<sub>2</sub>O<sub>3</sub>/SiC composite ceramics aid to decrease sintering temperature, simplest synthesis conditions, lower manufactured cost than SiC ceramic, higher thermal conductivity and bending strength also better thermal shock resistance compared with oxide ceramics (Xu *et al.*, 2016). Although these properties is an advantage to this composite but it limited in terms of limited virtual non- existence of a cheap and reliable way to prepare fully dense, defect free ceramic bodies with complex shapes and containing homogeneously distributed reinforcing (toughening) SiC inclusions (Galusek *et al.*, 2014).

### **2.3 Properties of Ceramic and Composite Ceramic**

Alumina and SiC were well studied their morphologies and phase stated from Bi *et al.*, 2014. Phase analyze were conducted by X-ray diffraction (XRD) (Asmi & Low, 2014). Microstructure was observed by scanning electron microscopy (SEM) (Yi *et al.*, 2014) and the porosity was measured by Archimedes method (Galusek *et al.*, 2014). Kim *et al.*, (2016) studied the flexural strength of the Alumina specimens and was measured through a 3-point bending test using a universal testing machine.

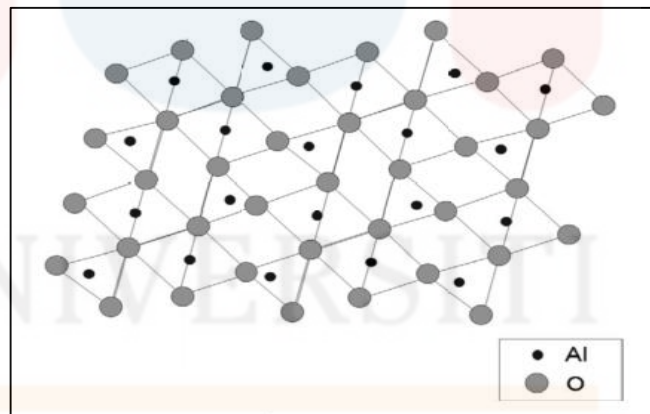
Despite the technique used, it aimed to produce high purity alumina because of its excellent structural, chemical and thermal stabilities (Li *et al.*, 2016). In the present

work, porous alumina substrate was fabricated via the sponge replication technique which divided into two stages, namely a substrate preparation step and dip-coating process to increase the properties (Jamaludin *et al.*, 2016). Other than sponge replication, porous such as powder or fiber sintering, plasma spraying, gas foaming, freeze casting, space-holder, and 3D rapid prototyping also was used (Wang *et al.*, 2016)

Silicon carbide fibers shown as excellent reinforcement candidate for high-temperature structural ceramic matrix composites due to the high strength and stability at high temperatures, low creep, high oxidation and corrosion resistance, high thermal conductivity and high thermal shock resistance (Yang *et al.*, 2013). From Metal (2006), SiC can be synthesized at the temperature higher than 1300°C by carbothermal reduction, and the amount of SiC increased with increasing treating temperature. While, via in-situ synthesize the pore distribution become more homogeneous (Xu *et al.*, 2014). They also found the carbothermal reduction method was used to in situ form Al<sub>2</sub>O<sub>3</sub> to bond with SiC for synthesizing Al<sub>2</sub>O<sub>3</sub>/SiC composites at 1540 °C. This proven by Sulaiman *et al.*, (2014) that instead of SiC which has higher melting point for casting, the composite of SiC-Al<sub>2</sub>O<sub>3</sub> also offers high susceptibility properties and can be formed at low temperature. While, porous ceramics offer a growing interest for multifunctional applications such as construction materials, biomaterials, materials for energy production and filtration (Staub *et al.*, 2016) be used in this composite by using sponge replication.

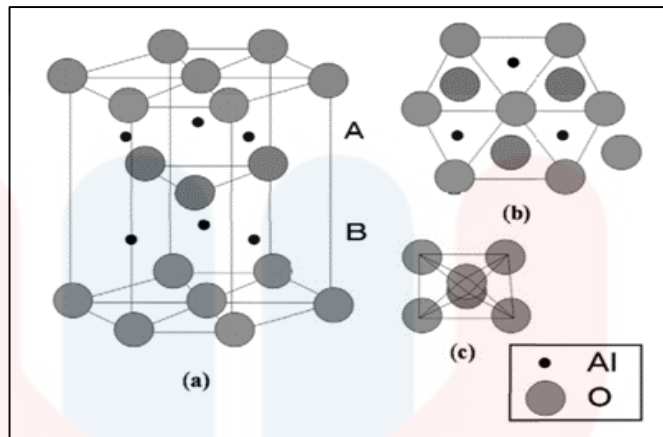
### 2.3.1 Phase Characterization

XRD studied was reported the single phase of Alumina formed by the synthesis of calcined bauxite (Li *et al.*, 2016). The Alumina synthesise from the bauxite because 80.9 wt% of bauxite is Alumina (Li *et al.*, 2016). XRD studied obtained from Metal (2016), had found the Al atoms exist in mullite,  $\text{Al}_2\text{O}_3$ , and amorphous phases at the treating temperatures under  $1700^\circ\text{C}$ , and only in  $\text{Al}_2\text{O}_3$  when treated at  $1700^\circ\text{C}$  can be found in the XRD pattern. Alumina can be from bauxite at specific sintering temperature. Alumina is a compound of FCC and lattice parameters was changed when nearest-neighboring atom around the vacancies was also different when Si vacancy formed and the formation energies of  $\text{V}_{\text{Si}}$  at 7.86 eV explained by Yang *et al.*, (2013). Alumina structure in Figure 2.1 may be two types of sites, hexagonal and octahedral in which it holds the atoms. Hexagonal sites are the corner atoms in the cell while the octahedral sites are present between two layers of vertical stacking (Davis, 2010).



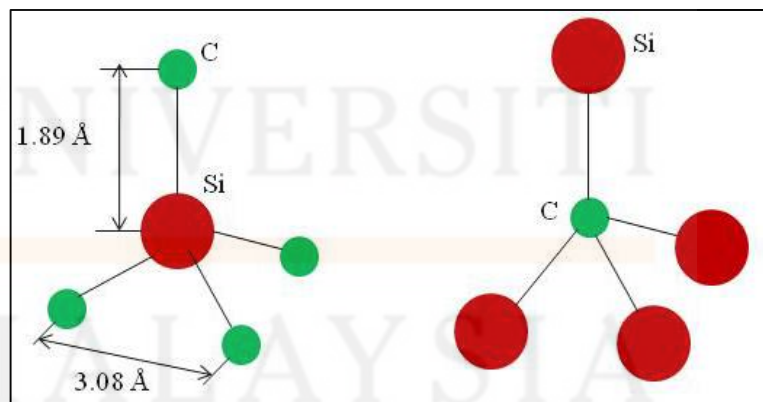
**Figure 2.1:** Structure of Alumina in which half of the Al ions are occupy tetrahedral sites (Shirai *et al.*, 2009)

This supported by the Shirai *et al.*, (2009) in Figure 2.2 crystal structure of  $\alpha$ - $\text{Al}_2\text{O}_3$ , which is called corundum structure, ideally consists of close packed planes (A and B planes) of large oxygen anions (radius 0.14 nm) stacked in the sequence



**Figure 2.2:** (a) Corundum structure of  $\alpha$ - $\text{Al}_2\text{O}_3$ , (b) Top view of the corundum structure, and (c) Octahedral structure of  $\alpha$ - $\text{Al}_2\text{O}_3$

From Duan *et al.*, (2014), SiC powders produced by carbothermal reduction reaction of  $\text{SiO}_2$ . It exhibited that the samples was pure and well crystallized  $\beta$ -SiC (Yang *et al.*, 2013). This proven by Li *et al.*, (2014) that the interplanar spacing of 0.25 nm agreed well with the (111) plane of  $\beta$ -SiC. Figure 2.3 show four Si(C) atoms are strongly bonded with  $\text{sp}^3$ -tetrahedral bond with C(Si) atoms. The distance between the carbon atoms is 3.08 Å and the distance between silicon and carbon atom is 1.89 Å (Sekhar, 2013).



**Figure 2.3:** Tetrahedral building block of SiC crystal. (a) Four carbon atoms bonded to one silicon atom (b) Four silicon atoms bonded to one carbon atom

### 2.3.2 Microstructure

Scanning electron microscopy (SEM) of Alumina ceramics was shown in the study by Li *et al.*, (2016) get almost fully dense microstructure and the alumina grains is generally round with diameter ranging from 0.2 to 0.4  $\mu\text{m}$ . In Li *et al.*, (2014) studied alumina sintered at 1550°C produced outer surface porosity of 11% and the sintered necks were formed between Alumina. Defects were observed as skeleton struts, fractured surface, and surface and within the skeleton strut by scanning Alumina. The elimination of defects, porosity reduction, appropriate sintering temperature, improved structural framework (Jamaludin *et al.*, 2016).

SEM of SiC spherical particles of 300 nm to 400 nm in diameter. The filament diameter of SiC fibers was about 15  $\mu\text{m}$  observed by SEM (Ye *et al.*, 2013). Yang *et al.*, (2013) research seen that the SiC powders was irregular shapes on order of several microns. The elongated SiC grains make quite a high contribution to toughening through crack deflection and crack- bridging (Bucevac, 2014).

### 2.3.3 Electromagnetic Absorption

Electromagnetic absorption in past research at the University of Florida focused primarily on high-temperature processing of materials, including microwave absorption/heating in composite susceptor materials (Clark *et al.*, 2000). Then, 3 years later, Yang *et al.*, (2013) found SiC powders enhanced microwave absorption coupled with improved broadband absorption, specifically increased microwave absorption properties at higher temperature.

Despite use of SiC which high cost on raw material, the composite of SiC/Al<sub>2</sub>O<sub>3</sub> was studied at different concentration (30, 40, 50, 60, 70 wt% SiC). From

Sulaiman *et al.*, (2014), slip casting processing method was applied. It found 40 wt% SiC/Al<sub>2</sub>O<sub>3</sub> crucible have high electromagnetic wave absorption which produced higher heat (350°C) within 10 minutes of microwave rays.

### 2.3.4 Density and Porosity

Apparent porosity (Pa) and bulk density (Db) of the composites were measured by the Archimedes Method (Xu *et al.*, 2014). 40 wt% SiC composite crucible displayed the optimum between the density and the porosity parameter which the density was 2.95 g/cm<sup>3</sup>, and the porosity was 21.4% (Sulaiman *et al.*, 2014).

$$\text{Bulk density, } \rho \left( \frac{\text{g}}{\text{cm}^3} \right) = \frac{D}{W-S} \times \rho_w \quad \text{Equation (2.1)}$$

$$\text{Apparent porosity, } \rho_d = \left( \frac{W-D}{W-S} \right) \times 100\% \quad \text{Equation (2.2)}$$

Where,

D = Dry weight

S = Saturated weight

S = Suspended weight

### 2.3.5 Dielectric Loss

Dielectric properties of the material compromised the understanding of the microwaves/materials interaction (Fagury-neto & Kiminami, 2001). The finding from Yin *et al.*, (2013) explained the induced electric current may be produced in the SiC matrix layer, and the dielectric loss considerably increased. Firing the composite at 1000°C produced high dielectric loss (0.09) at the high-frequency region. The firing at 1100°C result the highest dielectric loss at the lower-frequency region (0.04)



(Sulaiman *et al.*, 2014). The dielectric loss can be lessened by using microwave sintering because the heat generated internally through the interaction of the microwaves with the atoms, ions, and molecules of the material, which produces an inverse heating profile (Lakshmanan, n.d.).



## CHAPTER 3

### MATERIALS AND METHODS

#### 3.1 Experimental Process

This chapter explains the materials and methods that are planned to be conducted. The Silicon carbide and alumina powder will act as raw materials will be manipulating in term of their composition. The solid state reaction method will be conducted to produce the composite and then the future testing of microstructure, phase analysis, density and porosity measurement and electromagnetic will be continued. The sintering procedures will be conducted to improve the properties of porous alumina sponge replication technique. Figure 3.1 shows the processing of making the composite will use solid state reaction and follows the research.

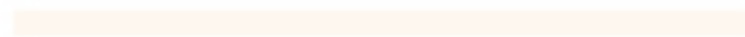
#### 3.2 Raw Materials Characterizations

To analyze the phase present, XRD will be used from  $10^\circ$  to  $90^\circ$  of diffraction angle.  $\text{Al}_2\text{O}_3$  and SiC will be tested using Bruker, 2D Phaser, Powder Diffractometer. For identification of X-Ray diffraction pattern, the DIFFRAC.EVA software will be used to compare the initial phases of both materials. The phases summaries in tables for both compositions. While, for microstructure analysis, Scanning Electron

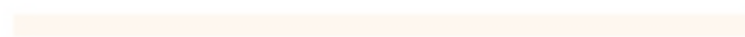
Microscope (SEM) will be used. The analysis will be explained well in term of its shape, defect, and microstructure size.



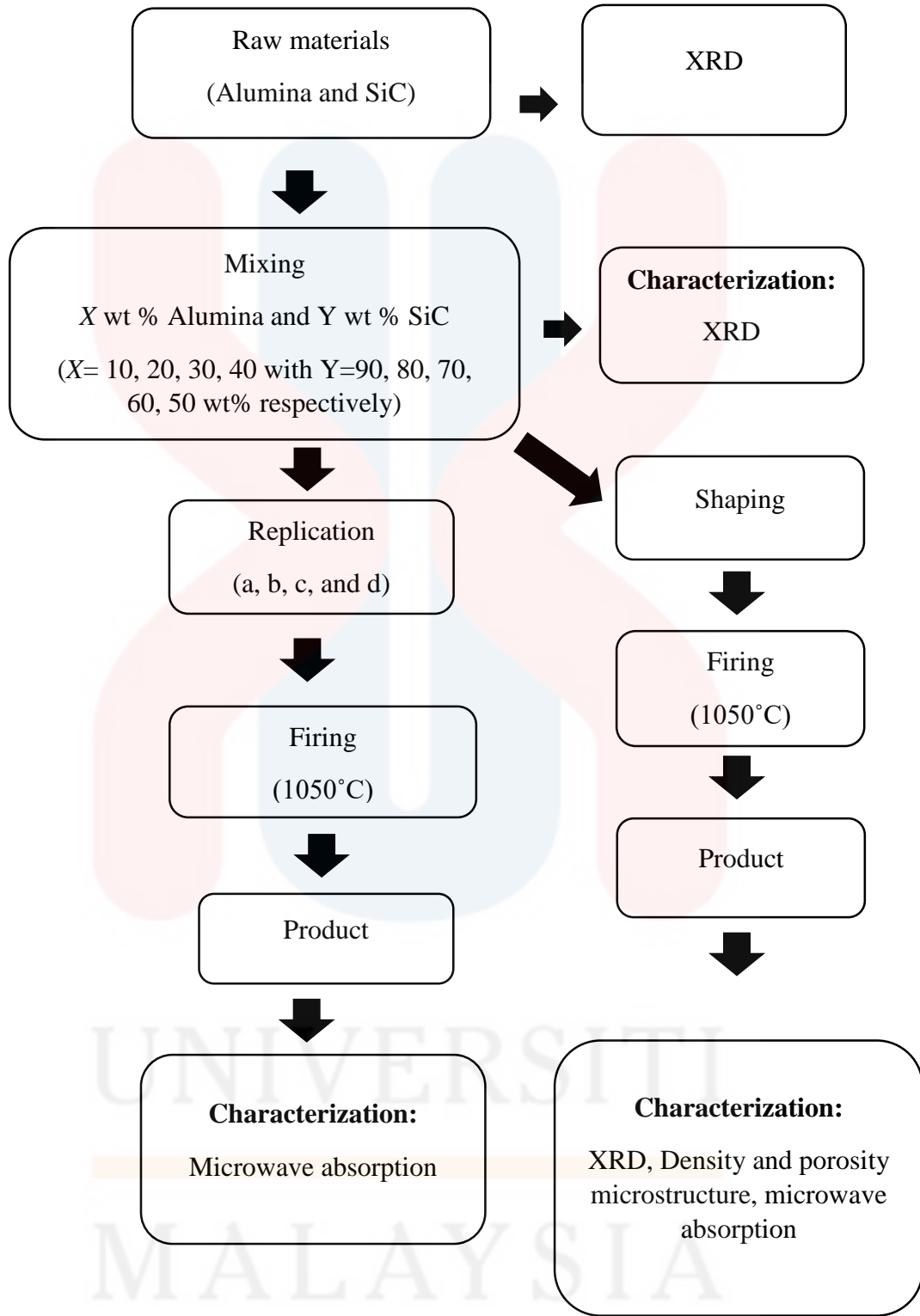
UNIVERSITI



MALAYSIA



KELANTAN



**Figure 3.1:** The research flow chart of SiC/Al<sub>2</sub>O<sub>3</sub> composition

### 3.3 Processing Methods

The processing of making the composite will use solid state reaction and follows the research flow chart in Figure 3.1. Alumina and silicon carbide powder will be testing using XRD, SEM and EM. The data collected will be the information to be compared with the process composite. Raw material of alumina powder and silicon carbide powder then will be weighted accurately for 5 compositions and will be mixed well in different beaker for each according to the Table 1. The samples of each composition then will be taken to XRD analysis. To make it slurry, the mixed powders will be added with 50 ml distilled water and stirred well using magnetic stirrer for an hour to make it achieve consistency. Then, the sponges (dimension of 3 cm×3 cm×3 cm) soak completely in the slurry. Then, the sponge squeezes and release to remove trap air bubble in the slurry before dried at room temperature for 48 h. Then, the sponges being put in a furnace for next 12 h in 1050°C for 5°C per minute of heating rate.

Green body form then ready for the testing. The sample of each testing will be prepared at definite dimension using diamond cutter. Lastly, the composite form will be study in term of XRD, SEM, Density and Porosity, EM and microstructure. The overall processing is in Figure 3.1.

**Table 3.1:** Composition of SiC/Al<sub>2</sub>O<sub>3</sub> Composite

Alumina Powder (wt%)	Silicon Carbide Powder (wt%)	Sample Code
10	90	10 wt% Al <sub>2</sub> O <sub>3</sub>
20	80	20 wt% Al <sub>2</sub> O <sub>3</sub>
30	70	30 wt% Al <sub>2</sub> O <sub>3</sub>
40	60	40 wt% Al <sub>2</sub> O <sub>3</sub>
50	50	50 wt% Al <sub>2</sub> O <sub>3</sub>

### 3.4 Material Characterizations

To determine the characteristic of the materials after it had been synthesized, material characterization has been characterizing in term of phase analysis, microstructure analysis, density and porosity measurement, and electromagnetic. The results then will be compared to other past researcher result.

#### 3.4.1 Phase Analysis (XRD)

All of the composition of SiC/Al<sub>2</sub>O<sub>3</sub> composite will be analysed using XRD. The software and database will be installed and peak search using software will be done. Then, the phase existence and crystal structure will be analyse using software DIFFRAC.EVA. and DIFFRAC.TOPAS.

### **3.4.2 Microstructure (Optical Microscope)**

In the study, using optical microscope, the morphology of the susceptor of SiC/Al<sub>2</sub>O<sub>3</sub> will be examined. All specimen will be prepared in pallet with dimension 6 mm in diameter. Then, using software, the structure will be analyzing and explained well compared to each composition.

### **3.4.3 Density and Porosity Measurement**

The samples prepared in rounded pallet form with the dimension of 6 mm in diameter. The weight of SiC/Al<sub>2</sub>O<sub>3</sub> composites will be measured and recorded. The air bubble trap will be removed using desiccator in the vacuum. The final weight in air of the composite will be measured and recorded. Then, the bulk density of samples will be calculate using the Equation 2.1 and the apparent porosity will be calculate using Equation 2.2.

### **3.4.4 Electromagnetic**

Crucibles as electromagnetic absorber will be put in the microwave. Using 700 watt of power, the electron will be radiated to the sample and using thermocouple, the heating rate for every half minute in 12 minute will be measure. The graph of temperature against time will be plotted.

### 3.4.5 Dielectric Properties

The crucibles will be put in the impedance analysis with range frequency (1MGz-1GHz). The analysis of dielectric loss will be conducted with the difference frequency. Graph of dielectric constant vs frequency and dielectric loss vs frequency will be plotted. The theory of dielectric loss increase with the increasing of electromagnetic absorption. The dielectric constant are calculate base on calculation in Equation 3.4, 3.5, and 3.6.

$$\text{Capacitance, } C = \epsilon_0 \left(\frac{A}{l}\right) \quad (\text{Equation 3.4})$$

$$\text{Capacitance, } C = \epsilon_r \epsilon_0 \left(\frac{A}{l}\right) \quad (\text{Equation 3.5})$$

$$\text{Dielectric Constants, } \epsilon_r = Cl/(\epsilon_0 \cdot A) \quad (\text{Equation 3.6})$$

Where,

A = Surface Area (m),

l = Length of Pellet (m),

$\epsilon_0$  = Universal Constants ( $8.85 \times 10^{-12}$ ).



## CHAPTER 4

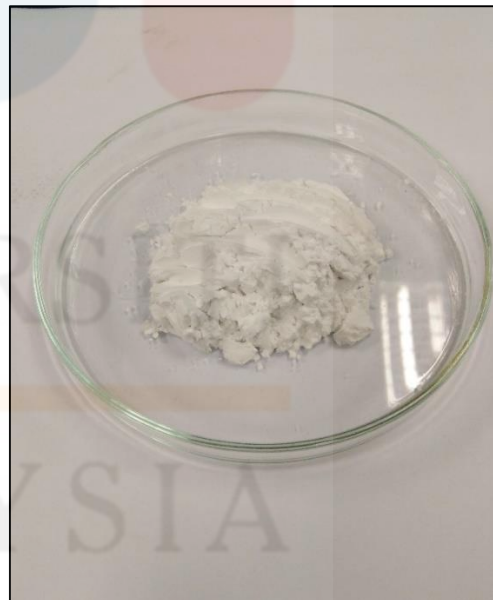
### RESULT AND DISCUSSION

#### 4.1 Introduction

The experiment was conducted in two separate parts. The first part was to determine the best composition of alumina and silicon carbide that used to make the composite. The second part was to find the best pore size for the porous susceptor synthesis. The manufactured alumina and silicon carbide powder were purchased from Sigma-Aldrich as the raw material as in Figure 4.1 and 4.2.



**Figure 4.1:** Silicon Carbide



**Figure 4.2:** Aluminium Oxide

XRD analysis conducted for the both of raw material, the mixed of each composition before sintering process and after sintering process. The other test conducted to find the best composition and then further for finding the best pore size

of sponge to be use as its replication. The sponge went to optical microscope to find the standard deviation of its pore size and the product test using microwave absorption testing to find the best size.

## **4.2 Raw Materials**

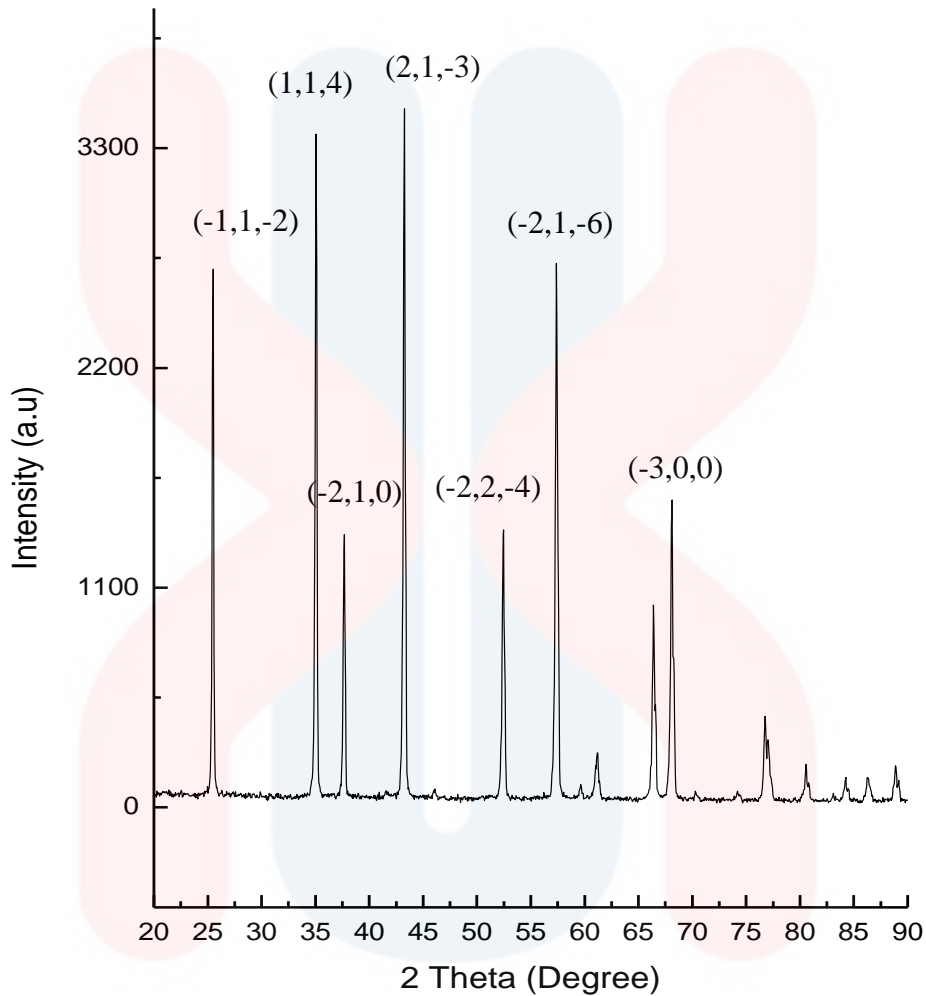
In this study, alumina and silicon carbide in powder form were used as raw materials for the both part while the second part added with 5 different pore size of sponges.

### **4.2.1 Characterization of Raw Materials**

Analysis conducted to characterize raw material is X-Ray Diffraction which the powder approximately 10 g used to characterize in term of its phase, lattice parameter and crystal structure. The characterization of raw material used as the references to any changes to the further process.

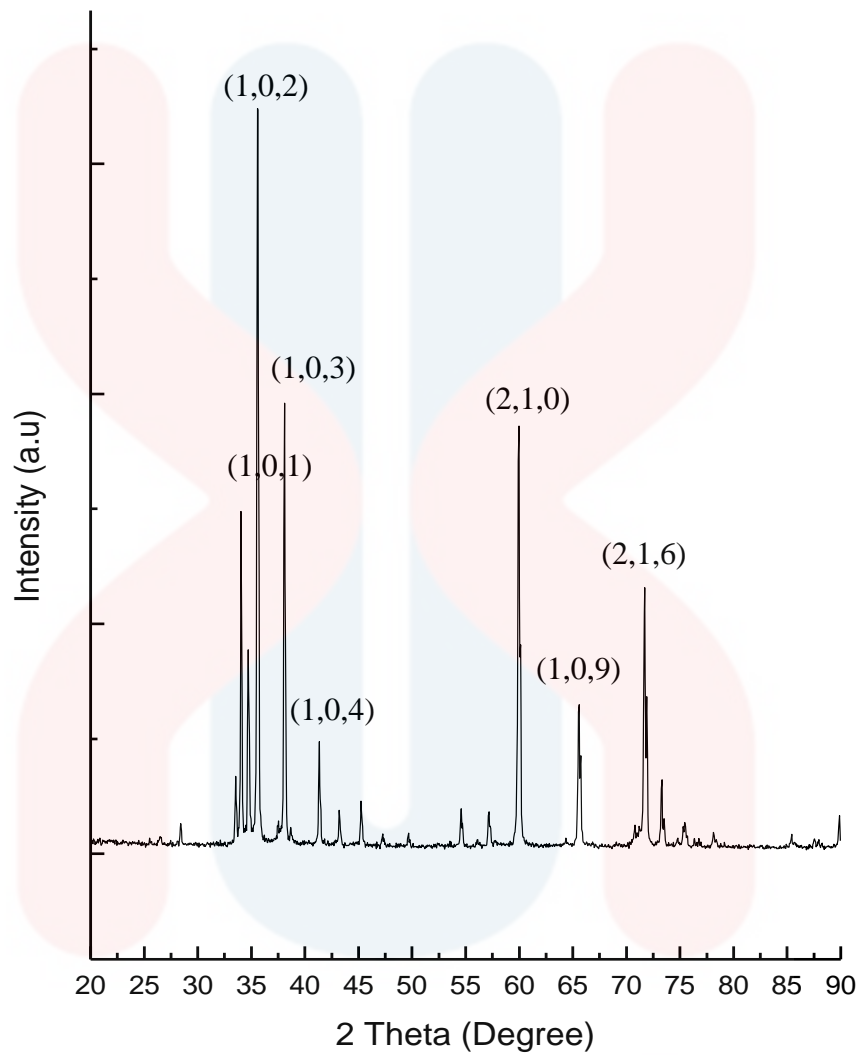
#### **4.2.1.1 X-ray Diffraction Analysis**

The raw material which is Alumina matched to the pattern of file COD 9009671 (Appendix F). Seven peaks identified closely matched with the standard diffraction pattern of Alumina. The peaks known as Alumina at the intensity of higher than 1100 a.u produce Miller Indices of (-1,1,-2), (1,1,4), (2,1,0), (2,1,-3), (2,2,-4), (-2,1,-6), (-3,0,0). The hexagonal closed-packed or hcp crystal structure detected in the Alumina or its mineral name is Corundum.



**Figure 4.3:** XRD Pattern of  $\text{Al}_2\text{O}_3$  (COD 9009671)

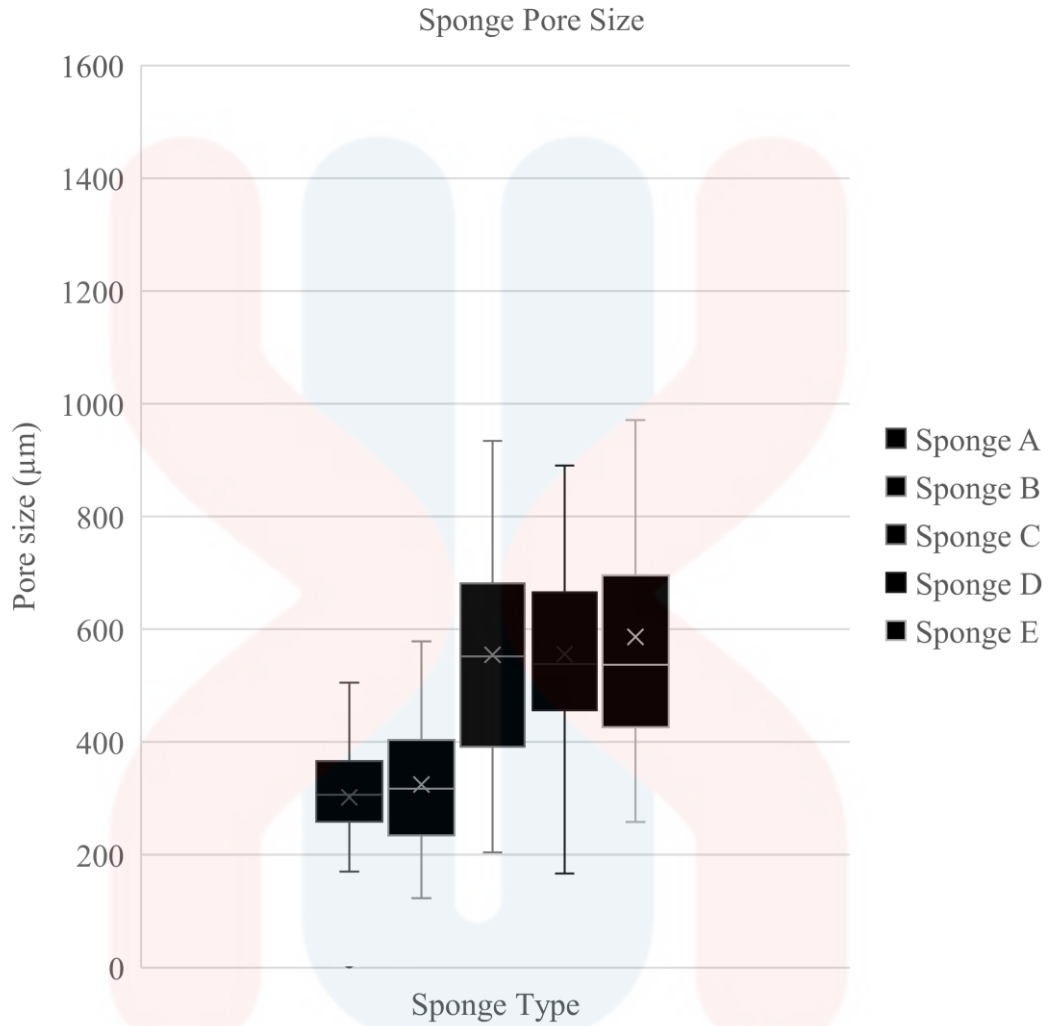
The raw material which is Silicon Carbide (SiC) matched to the pattern of file COD 1011053. Seven peaks identified closely matched with the standard diffraction pattern of SiC. The peaks known as SiC at the intensity of higher than 1100 a.u produce Miller Indices of (1,0,1), (1,0,2), (1,0,3), (1,0,4), (2,1,0), (1,0,9), (2,1,6). The hexagonal closed-packed or hcp crystal structure detected in the C Si of Moissanite 6H. The distance of carbon atom is same to the *Sekhar, 2013* at 3.08 Å but the distance between silicon and carbon atom is 1.48 Å differ to his at 1.89 Å.



**Figure 4.4:** XRD Pattern of SiC (COD 1011053)

#### 4.2.1.2 Microstructure of Sponge

Optical microscope was used to identify the microstructure of sponge. Using computer software, statistical analysis has been done to measure their pore size. Sponge A, B, C, D and E as shown in Figure 4.5 have average pore size of 95.346, 117.624, 191.952, 204.057, 240.609  $\mu\text{m}$  respectively.

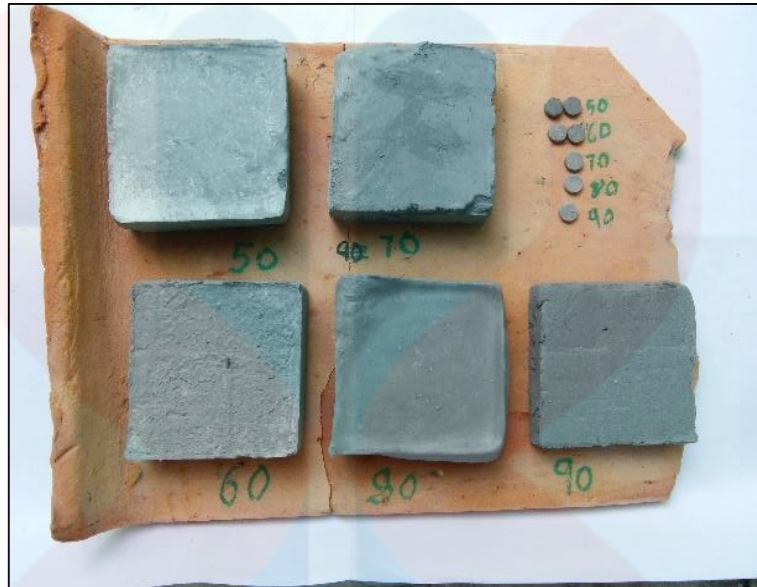


**Figure 4.5:** Sponge pore size

### 4.3 Mixing Process

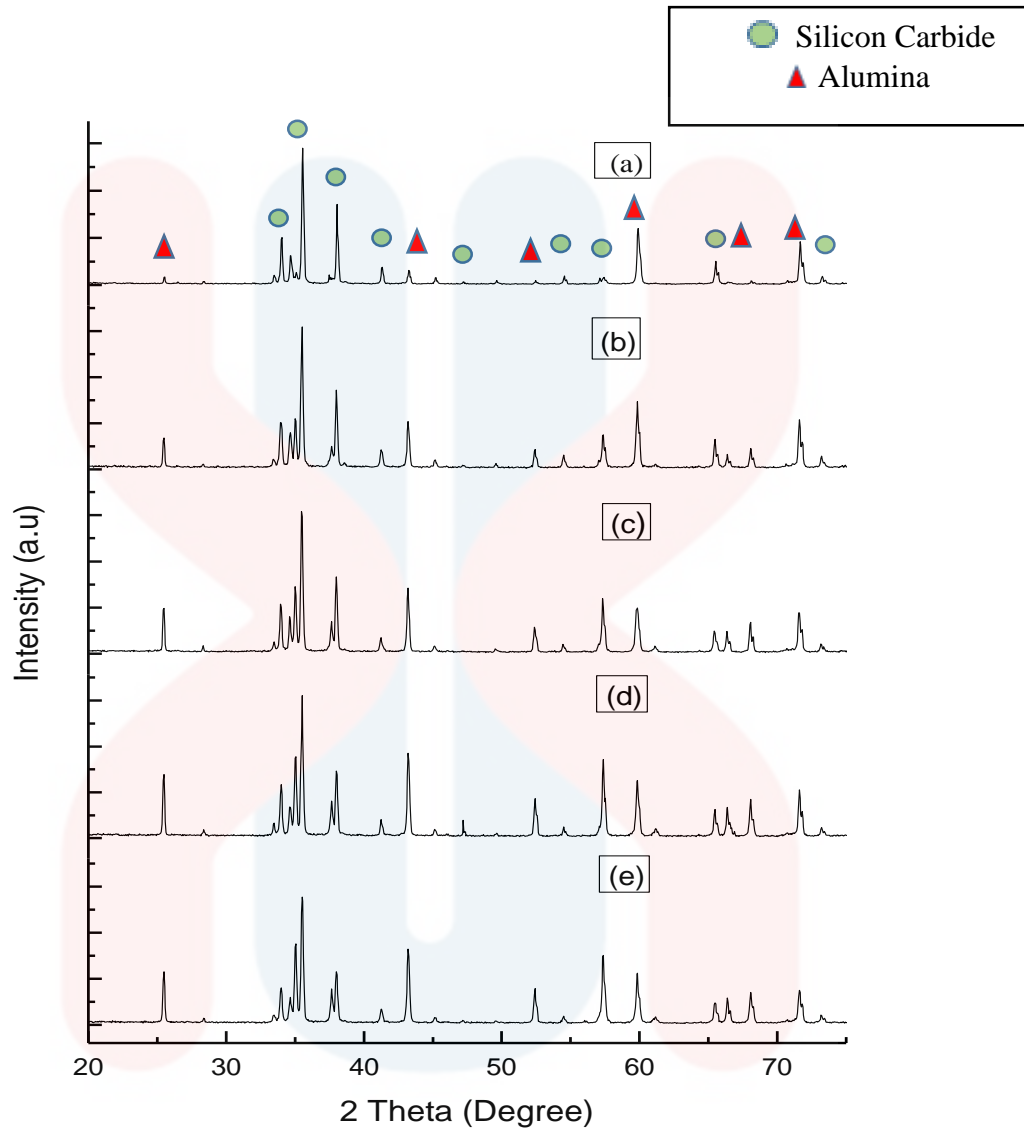
The mixture of this two material with different ratio added with distilled water form slurry. The slurry mix well using magnetic stirrer on a hot plate at 800 rpm for one hour for each composition. This well mix slurry pours in POP mould produce rectangular composite. The excess was dry and make pallets of each are 0.11 g to use

in the testing and the other excess went to the characterization process of composite before sintering process.



**Figure 4.6:** The composite before sintering process

The result shown in Figure 4.7 extracted from Diffract.Eva software. The first peak of both five graphs is alumina which is highest at the 50 wt%  $\text{Al}_2\text{O}_3$  while lowest at the 10 wt %  $\text{Al}_2\text{O}_3$ . The highest peak also indicates from  $40^\circ$  to  $50^\circ$  which is highest at the first sample and lesser to the other sample. The sample matches the file COD 9009671 and COD 1011053 which refer to the identification of alumina and silicon carbide present in the composite.



**Figure 4.7:** XRD pattern of SiC/Al<sub>2</sub>O<sub>3</sub> composite after mixing process, (a) 50 wt% SiC/Al<sub>2</sub>O<sub>3</sub>, (b) 40 wt% SiC/Al<sub>2</sub>O<sub>3</sub>, (c) 30 wt% SiC/Al<sub>2</sub>O<sub>3</sub>, (d) 20 wt% SiC/Al<sub>2</sub>O<sub>3</sub>, (e) 10 wt% SiC/Al<sub>2</sub>O<sub>3</sub>

#### 4.4 Composite Product

All shaped composite dried up in room temperature for 24 hours before sinter at 1050 °C in furnace for 12 hours with 5 °C per minute of heating and cooling rate. The product cleans gently using cotton prepared for the testing. The composite place

on a traditional ceramic product for the sintering process to avoid the contamination.

The Figure 4.8 show the composite after the sintering process.



**Figure 4.8:** The composite after sintering process

#### **4.4.1 Characterization of Composite Product**

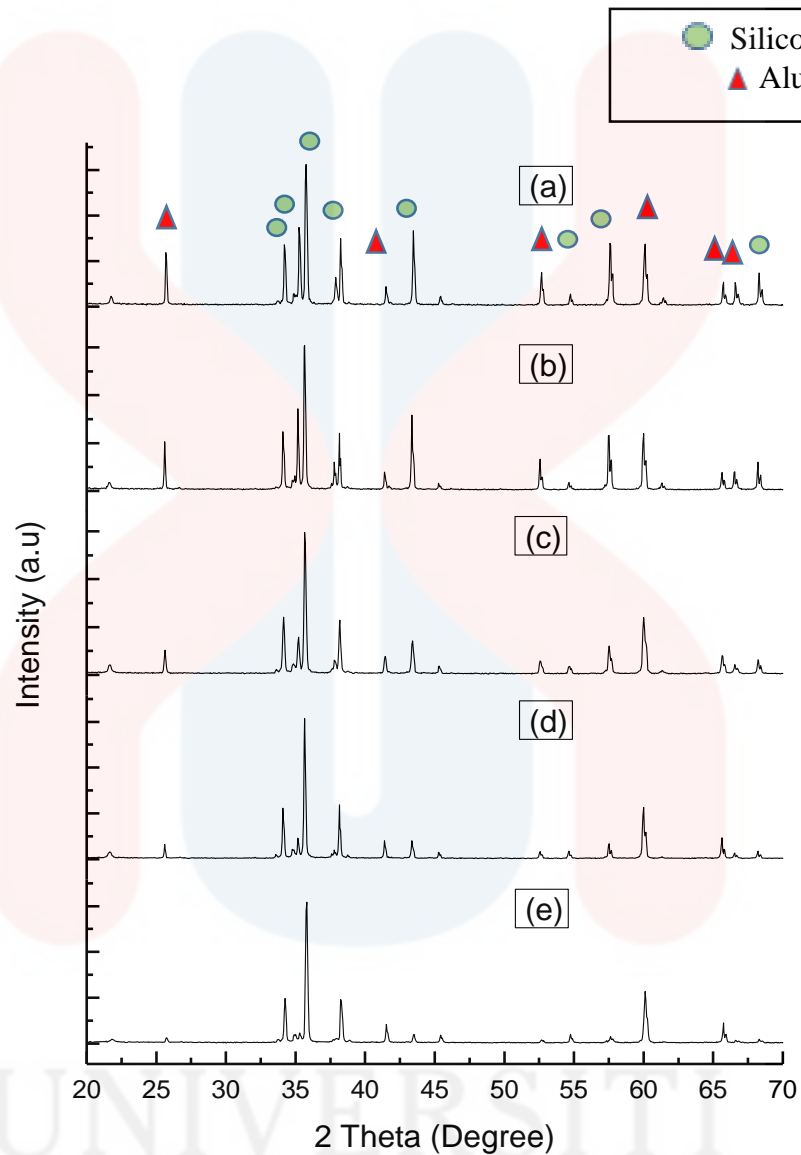
Analysis conduct to characterize composite after it have been sinter for 12 hours in furnace of 1050 °C with 5 °C per minute characterize from X-Ray Diffraction analysis, density and electromagnetic absorption to find the best composition.

##### **4.4.1.1 X-Ray Diffraction analysis**

The result shown in Figure 4.8 shows sample (a) are highest with the Alumina while sample (e) show lowest content of Alumina. In term of Silicon Carbide content, the sample (a) have high distribution compare to sample (e) although sample (e) have higher content of Silicon Carbide. This is because sample (a) is stable in the firing and Alumina able to be a good filler between the Silicon Carbide. While the other sample



did not show are showing the Silicon Carbide at high peak but its not as many as sample (a).

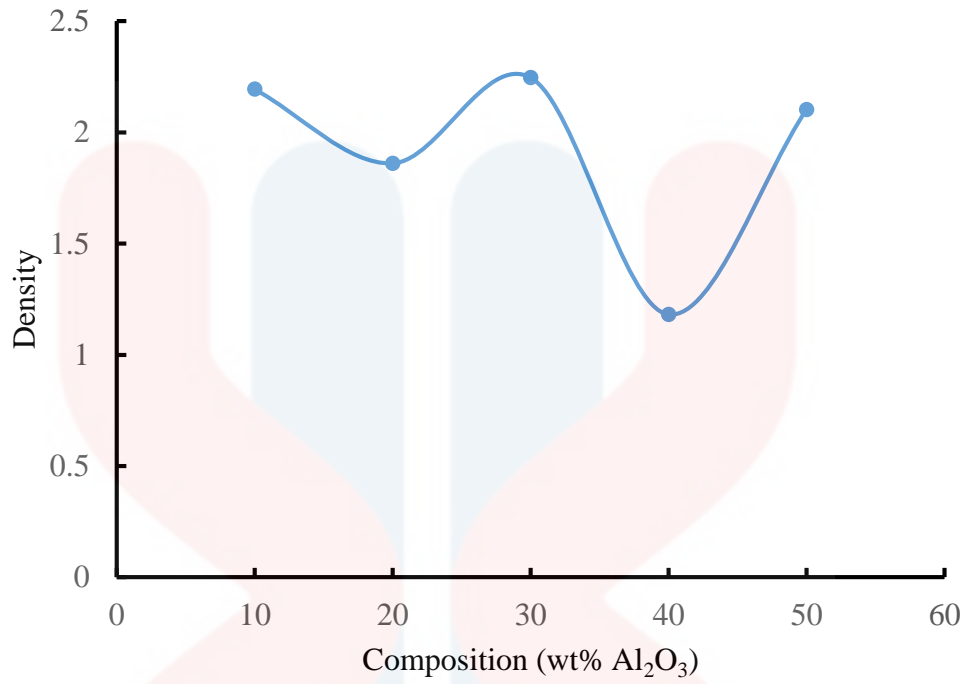


**Figure 4.9:** XRD pattern of SiC/Al<sub>2</sub>O<sub>3</sub> composite sintering process, (a) 50 wt% SiC/Al<sub>2</sub>O<sub>3</sub>, (b) 40 wt% SiC/Al<sub>2</sub>O<sub>3</sub>, (c) 30 wt% SiC/Al<sub>2</sub>O<sub>3</sub>, (d) 20 wt% SiC/Al<sub>2</sub>O<sub>3</sub>, (e) 10 wt% SiC/Al<sub>2</sub>O<sub>3</sub>

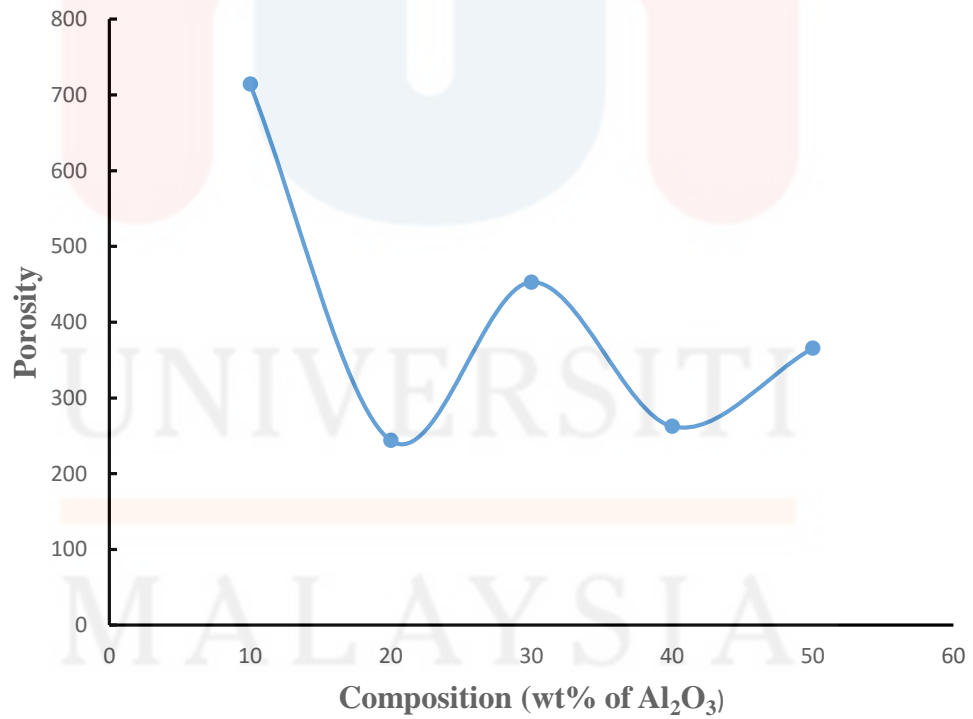
#### 4.4.1.2 Density and Porosity

The density of pallets after sintering is calculated as in equation 1 and 2 base on the reading and average of each composition referring to Appendix C and D. Bulk density and apparent porosity considered in both because the composite has porous structure which come from dry weigh, suspended and saturated. The values of each taken three time and the average calculated for each sample. The graph of bulk density and apparent porosity against weight percentage or sample code plotted in different graph. The graph shows the value of weight percentage of  $\text{Al}_2\text{O}_3$  from 10 % to 50 %, that is from 1.62 to 2.34  $\text{g}/\text{cm}^3$ . The sample of 10% and 30 % of  $\text{Al}_2\text{O}_3$  have higher bulk density. However, the sample which contain 20 % and 40 % of  $\text{Al}_2\text{O}_3$  resulting lower in term of bulk density. The value may be inaccurate due to undistributed applied force during the hand press process that effect the pressure applied or shaping process.

The second graph which is apparent porosity against weight percentage produce same trend to the bulk density. The apparent porosity produces from 160 to 720 % for the sample of 10 % to 50 % of  $\text{Al}_2\text{O}_3$ .



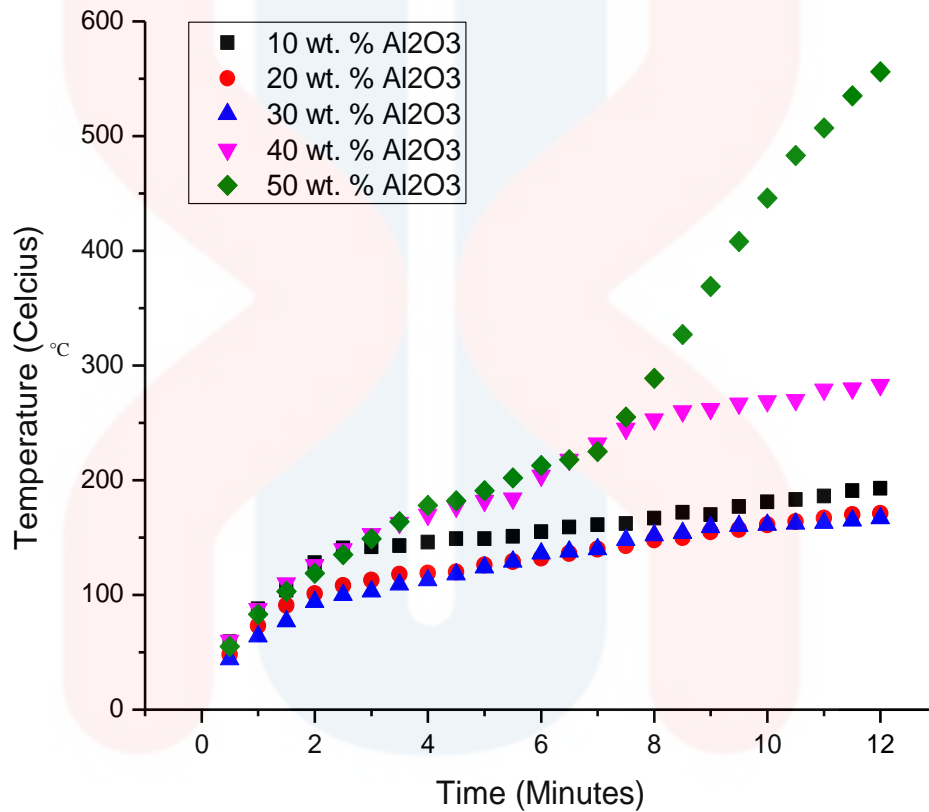
**Figure 4.10:** The density of composite with different composition



**Figure 4.11:** The porosity of composite with different composition

#### 4.4.1.3 Electromagnetic Absorption

The temperature for every half minute in 12 minutes taken and tabulated as in Appendix E and graph to indicate the trend are sketch.



**Figure 4.12:** The electromagnetic absorption with time of composite

The sample for 10 wt% Al<sub>2</sub>O<sub>3</sub> increases faster at the first 2 minutes and increase slowly for the next 10 minutes. The sample reached 193°C at minute of 12. There is slightly decreasing at minutes of 9. This indicate as the sample try to equilibrate its temperature to the surrounding in the microwave or the heat absorb by the base in the microwave. At minute of 4.5 to 5 and 7 to 7.5 the temperature is constant due to the upper of the sample assume to homogenously heated. The heat then distributes to the other part of the sample and the heat increases again.

The sample of 20 wt%  $\text{Al}_2\text{O}_3$  show increases from the start until minutes of 12 and constant at minute of 4 to 4.5. The sample increases faster at the first 3 minute and slowly increases for the next 9 minutes.

While 30 wt%  $\text{Al}_2\text{O}_3$  sample show differ trend with constantly increases from the start to the minutes of 9. The sample increase slight at minute of 9 to 12. This phenomenon is good as a susceptor that indicate to homogeneously heated and stable to be use. But the temperature still low for the limited time.


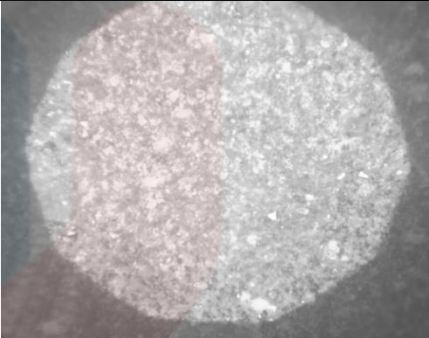
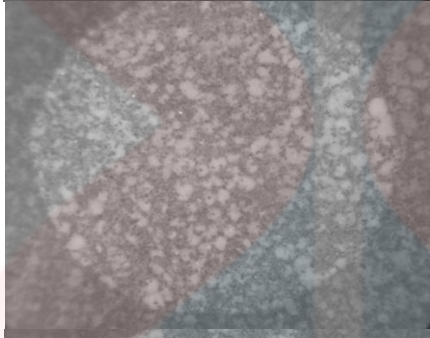

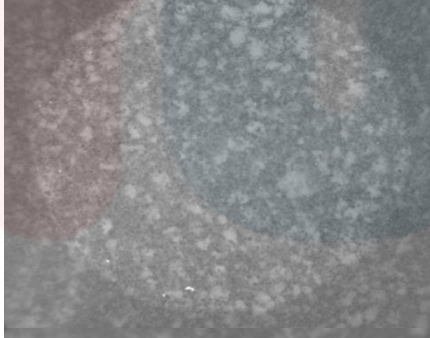
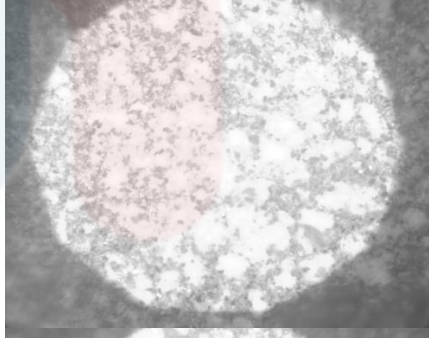
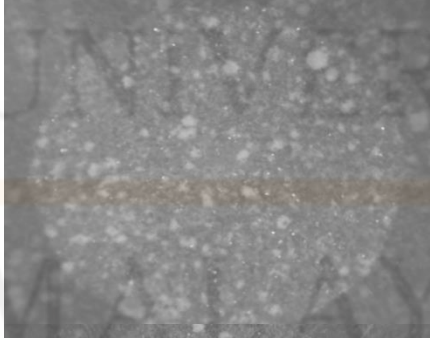
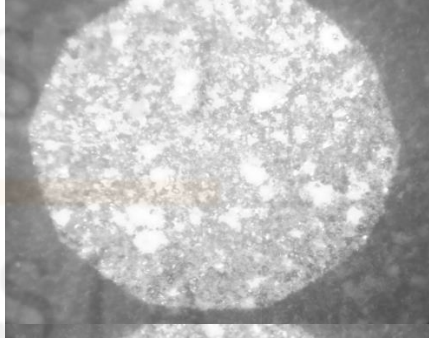
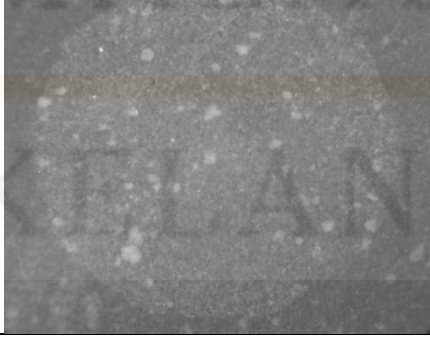
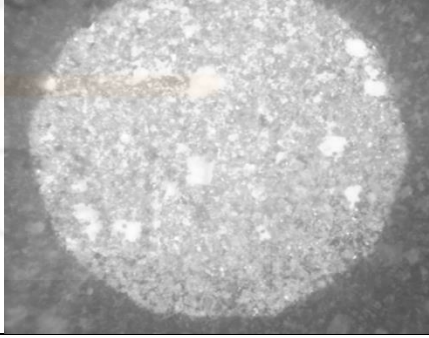
The 40 wt%  $\text{Al}_2\text{O}_3$  sample show better trend with increases constantly from the start until minutes of 11 and show to be constant at minutes of 11. The temperature reaches up to  $283^\circ\text{C}$  and the sample heated smoothly as a whole. This show the sample be able to heated homogeneously and good as a susceptor.

The 50 wt%  $\text{Al}_2\text{O}_3$  sample show fastest in temperature increases which reach up to almost  $600^\circ\text{C}$  in 12 minutes. The sample which contain same ratio of the SiC and  $\text{Al}_2\text{O}_3$  shows the ability to reach highest temperature among the other ratio and most stable which increases slowly at first then able to increase faster from the minute of 7 to 12.

#### 4.4.1.4 Microstructure

The sintered composite microstructure analyzes using optical microscope under magnification of 5 X and 10 X. The microstructure of 10 wt%  $\text{Al}_2\text{O}_3$  produce finer structure which the distribution of raw materials is structurally together. The grain is lesser and smaller in size than other sample produce after sintering process. The sample which contain higher alumina content tend to have large hole in its microstructure which may produce composite which poor in mechanical test.

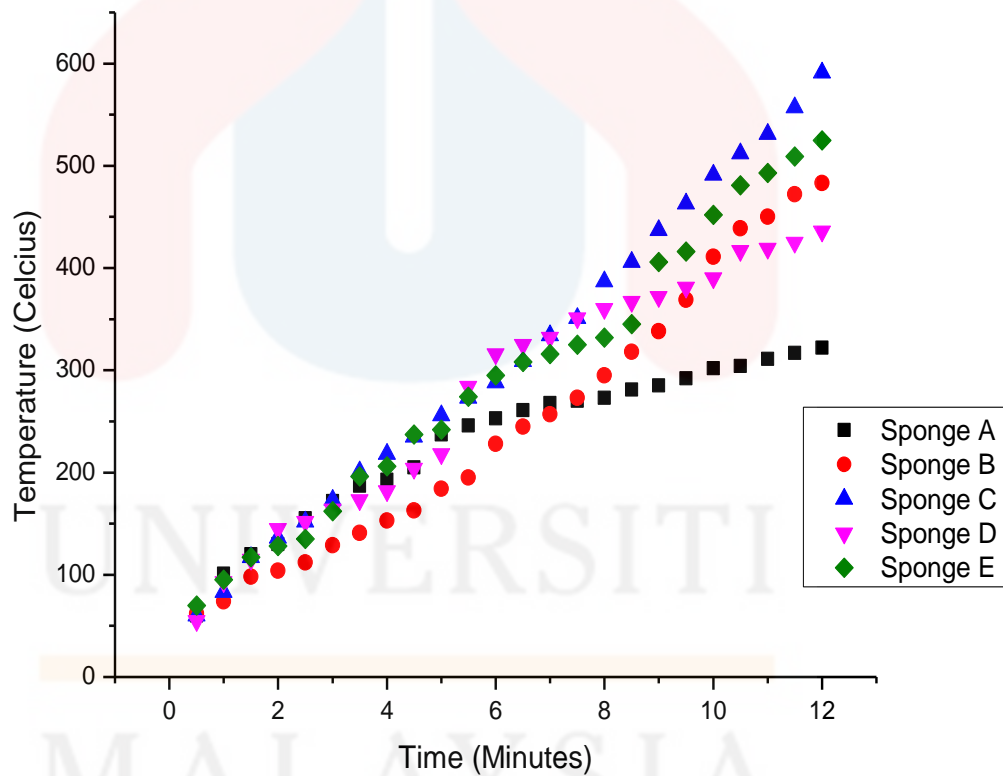
**Table 4.1:** The microstructure of sintered composite

Sample Code	5 X	10 X
10 wt% Al <sub>2</sub> O <sub>3</sub>		
20 wt% Al <sub>2</sub> O <sub>3</sub>		
30 wt% Al <sub>2</sub> O <sub>3</sub>		
40 wt% Al <sub>2</sub> O <sub>3</sub>		
50 wt% Al <sub>2</sub> O <sub>3</sub>		

#### 4.5 Porous Composite Product

All shaped composite dried up in room temperature for 24 hours before sinter at 1050 °C in furnace for 12 hours with 5 °C per minute of heating and cooling rate. The composite place on a traditional ceramic product for the sintering process to avoid the contamination.

##### 4.5.1 Electromagnetic Absorption



**Figure 4.13:** The electromagnetic absorption with time of porous composite using different sponge pore size

The temperature for every half minute in 12 minutes taken and tabulated as in Appendix H and graph to indicate the trend are sketch.

The sample for Sponge A show the lowest of temperature increasing that reach  $322^{\circ}\text{C}$  at minute of 12. There is sudden increasing g at minutes of 5 which indicate as the sample equilibrate its temperature to the surrounding in the microwave.

The sample of Sponge B show slow increases from the start until minutes of 10 and increase rapidly at minute of 10 to 12. While sample of Sponge C show differ trend with constantly increases from the start to the minutes of 12. The sample increase rapidly and reach highest temperature in 12 minute among 5 sponge pore size which is at  $591^{\circ}\text{C}$ . This phenomenon is good as a susceptor that indicate to homogeneously heated and stable to be use.

For sample of sponge D, there is rapid increase from minute of 5 to 6 and the trend increases throughout the time. This same to sample of Sponge E where rapid increases detected at minute of 9 to 10.

Among the 5 sponge, sponge C produce good absorption and this chosen as ideal pore size for the sponge replication of porous composite product.



## CHAPTER 5

### CONCLUSION AND RECOMMENDATION

#### 5.1 Conclusion

In conclusion, different ratio of Alumina produces different properties to the making does not lower the microwave absorption but increase the absorption in less time with the 50 wt% of Alumina. This study has two part, first part proven the ratio for the best microwave absorption while the second part proven the pore size that is the optimum to be used to produce porous susceptor.

The first part proven the 50 wt% of Alumina be able to absorb microwave ray up to 556°C in 12 minutes. This ratio gives out highest temperature and at once the density and porosity are the best after sintering process. The second part proven X pore size of 191.9523  $\mu\text{m}$  is the best to cope with the microwave ray, absorb and aid for sintering process.

In short, the porous suceptor is better compare to bulk susceptor and the Alumina is good to be fillers and decrease the temperature to heat up the susceptor in a microwave uses.

In short, the porous suceptor is better compare to bulk susceptor and the Alumina is good to be fillers and decrease the temperature to heat up the susceptor in a microwave uses.

## 5.2 Recommendation

There are few suggestion of experiment to be recommend to other researchers and academic members for further studies in porous susceptor field. First of all, the characterization of the composite can be made in term of mechanical properties which are not conducted in this studies. The mechanical important as the susceptor are exposed to handling activities. Next, the porous susceptor structure can be determine by using optical microscope (OM) for clear structure in distribution of material in a composite. Then, the raw material is not fix to Alumina but it can also be replacing with titanium or feldspar which have good conductive properties.

There also some steps to be consider in the experiment. This including the raw materials must be mix well into homogeneous slurry so that better and accurate results can be obtained.

## REFERENCES


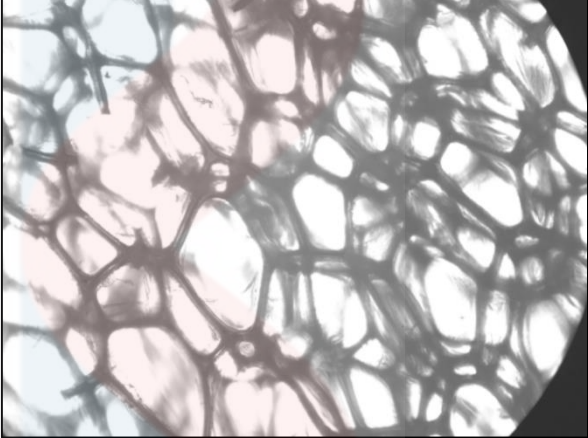

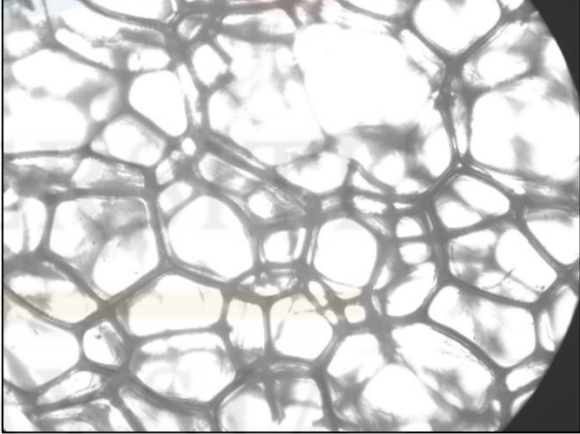
- Aeronautics, N. (n.d.). Silicon Carbide (SiC) Fiber- Reinforced SiC Matrix Composites.
- Alford, T. L., Gadre, M. J., Vemuri, R. N. P., & Theodore, N. D. (2012). Susceptor-assisted microwave annealing for activation of arsenic dopants in silicon. *Thin Solid Films*, 520(13), 4314–4320.
- Asmi, D., & Low, I. M. (2014). 6 - *Manufacture of graded ceramic matrix composites using infiltration techniques. Advances in ceramic matrix composites*. Woodhead Publishing Limited.
- Badiger, R. I., Narendranath, S., & Srinath, M. S. (2015). Joining of Inconel-625 alloy through microwave hybrid heating and its characterization. *Journal of Manufacturing Processes*, 18, 117–123.
- Bhattacharya, M., & Basak, T. (2016). A review on the susceptor assisted microwave processing of materials. *Energy*, 97, 306–338.
- Bucevac, D. (2014). *Heat treatment for strengthening silicon carbide ceramic matrix composites. Advances in Ceramic Matrix Composites*. Woodhead Publishing Limited.
- Carvalho, M. A., Calil Júnior, C., Savastano Junior, H., Tubino, R., & Carvalho, M. T. (2008). Microstructure and mechanical properties of gypsum composites reinforced with recycled cellulose pulp. *Materials Research*, 11(865), 391–397.
- Chen, L., Tang, C. Y., Ku, H. S. L., Tsui, C. P., & Chen, X. (2014). Microwave sintering and characterization of polypropylene/multi-walled carbon nanotube/hydroxyapatite composites. *Composites Part B: Engineering*, 56, 504–511.
- Clark, D. E., Folz, D. C., & West, J. K. (2000). Processing materials with microwave energy. *Materials Science and Engineering: A*, 287(2), 153–158.
- Cooke, T. F. (1991). Inorganic Fibers- A Literature Review. *Journal of the American Ceramic Society*, 78(12), 2959–2978.
- Davis, K. (2010). Material Review: Alumina (Al<sub>2</sub>O<sub>3</sub>). *School of Doctoral Studies European Union Journal*, 109–114.
- De Genua, F., & Sglavo, V. M. (2011). High strength engineered alumina-silicon carbide laminated composites by Spark Plasma sintering. *Procedia Engineering*, 10, 2621–2626.
- Deng, S., Djukic, L., Paton, R., & Ye, L. (2015). Thermoplastic-epoxy interactions and their potential applications in joining composite structures - A review. *Composites Part A: Applied Science and Manufacturing*, 68, 121–132.
- Duan, W., Yin, X., Li, Q., Schlier, L., & Greil, P. (2016). A review of absorption properties in silicon-based polymer derived ceramics. *Journal of the European Ceramic Society*, 1–9.
- Fagury-neto, E., & Kiminami, R. H. G. A. (2001). Al<sub>2</sub>O<sub>3</sub> / mullite / SiC powders synthesized by microwave-assisted carbothermal reduction of kaolin, 27, 815–819.
- Galusek, D., Sedláček, J., Klement, R., & Švančárek, P. (2014). *Silicon carbide-containing alumina nanocomposites: processing and properties. Advances in Ceramic Matrix Composites*.
- Heuguet, R., Marinell, S., Thuault, A., & Badev, A. (2013). Effects of the susceptor dielectric properties on the microwave sintering of alumina. *Journal of the American Ceramic Society*, 96(12), 3728–3736.


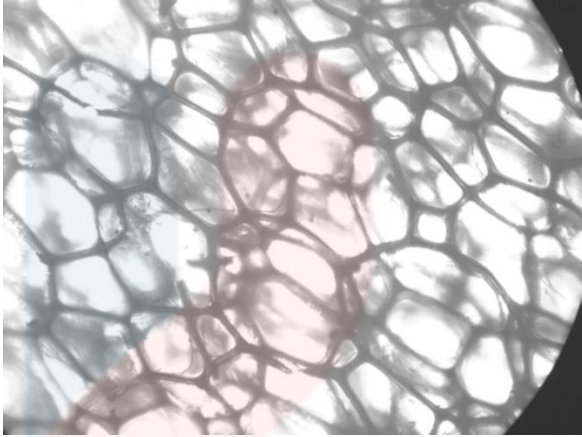

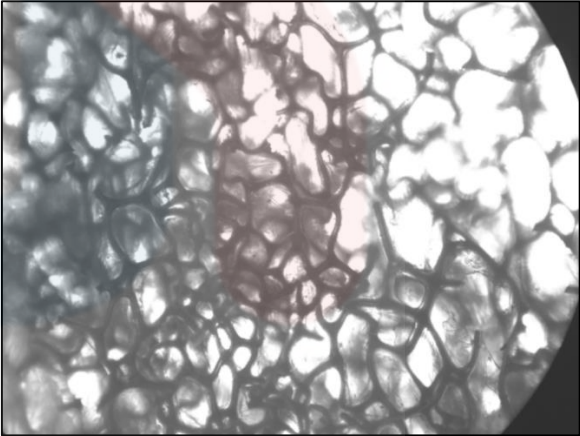

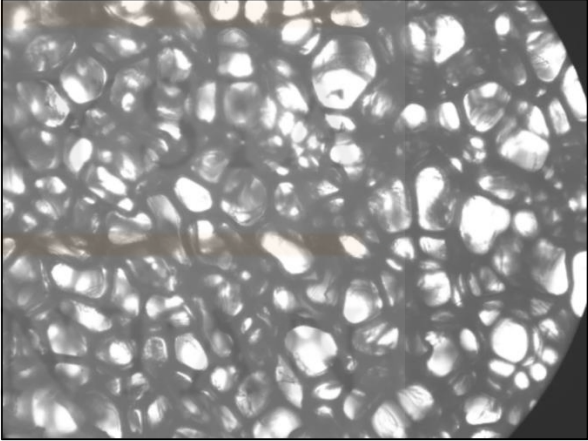
- Jamaludin, A. R., Kasim, S. R., Abdullah, M. Z., & Ahmad, Z. A. (2016). Physical, mechanical, and thermal properties improvement of porous alumina substrate through dip-coating and re-sintering procedures. *Ceramics International*.
- Kurşun, A., Bayraktar, E., & Enginsoy, H. (2016). Experimental and Numerical Study of Alumina Reinforced Aluminium Matrix Composites: Processing, Microstructural Aspects and Properties. *Composites Part B*.
- Lakshmanan, A. (n.d.). *SINTERING OF CERAMICS – NEW EMERGING* Edited by Arunachalam Lakshmanan.
- Leong, W., Wong, E., & Gupta, M. (2015). Using Microwave Energy to Synthesize Light Weight/Energy Saving Magnesium Based Materials: A Review, 1–18.
- Li, F., Liu, Z., & Sun, T. (2016). High temperature monitoring of silicon carbide ceramics by confocal energy dispersive X-ray fluorescence spectrometry. *Nuclear Instruments and Methods in Physics Research Section B: Beam Interactions with Materials and Atoms*, 373, 91–97.
- Li, L., Chen, M., Dong, Y., Dong, X., Cerneaux, S., Hampshire, S., ... Liu, J. (2016). A low-cost alumina-mullite composite hollow fiber ceramic membrane fabricated via phase-inversion and sintering method. *Journal of the European Ceramic Society*.
- Mandal, P. R., & Nath, T. K. (2014). Enhanced magnetocapacitance and dielectric property of  $\text{Co}_{0.65}\text{Zn}_{0.35}\text{Fe}_2\text{O}_4\text{-PbZr}_{0.52}\text{Ti}_{0.48}\text{O}_3$  magnetodielectric composites. *Journal of Alloys and Compounds*, 599, 71–77.
- Mendoza-Duarte, J. M., Estrada-Guel, I., Carretero-Gallardo, C., & Martínez-Sánchez, R. (2015). Study of Al composites prepared by high-energy ball milling; Effect of processing conditions. *Journal of Alloys and Compounds*, 1–6.
- Mu, Y., Zhou, W., Hu, Y., Wang, H., Luo, F., Ding, D., & Qing, Y. (2015). Temperature-dependent dielectric and microwave absorption properties of SiC/f, SiC-Al<sub>2</sub>O<sub>3</sub> composites modified by thermal cross-linking procedure. *Journal of the European Ceramic Society*, 35(11), 2991–3003.
- Naga, S. M. (2014). *Ceramic matrix composite thermal barrier coatings for turbine parts*. *Advances in Ceramic Matrix Composites*. Woodhead Publishing Limited.
- Osada, T., Nakao, W., Takahashi, K., & Ando, K. (2014). *Self-crack-healing behavior in ceramic matrix composites*. *Advances in Ceramic Matrix Composites*. Woodhead Publishing Limited.
- Rybakov, K. I., Olevsky, E. A., & Krikun, E. V. (2013). Microwave sintering: Fundamentals and modeling. *Journal of the American Ceramic Society*, 96(4), 1003–1020.
- Sekhar, V. C. (2013). A new approach for transition metal free magnetic SiC: Defect induced magnetism after self-ion implantation.
- Shirai, T., Watanabe, H., Fuji, M., & Takahashi, M. (2009). Structural properties and surface characteristics on aluminium oxide powders. *Annual Report of the Ceramics Research Laboratory Nagoya Institute of Technology*, 9, 23–31.
- Srivastava, N., & Chaudhari, G. P. (2016). Strengthening in Al alloy nano composites fabricated by ultrasound assisted solidification technique. *Materials Science and Engineering A*, 651, 241–247.
- Staub, D., Meille, S., Le Corre, V., Rouleau, L., & Chevalier, J. (2016). Identification of a damage criterion of a highly porous alumina ceramic. *Acta Materialia*, 107, 261–272.
- Sulaiman, M. A., Hutagalung, S. D., Ahmad, Z. A., Mohamed, M., Yusof, M., & Mamat, S. (2014). Enhanced Electromagnetic Absorption on Formulated SiC-Al<sub>2</sub>O<sub>3</sub> Composite Crucible, 2, 1–3.

- Sun, Z., Lu, C., Fan, J., & Yuan, F. (2016). Porous silica ceramics with closed-cell structure prepared by inactive hollow spheres for heat insulation. *Journal of Alloys and Compounds*, 662, 157–164.
- Wang, C., Chen, H., Zhu, X., Xiao, Z., Zhang, K., & Zhang, X. (2016). An improved polymeric sponge replication method for biomedical porous titanium scaffolds. *Materials Science and Engineering: C*.
- Xia, Z., & Li, L. (2014). Understanding interfaces and mechanical properties of ceramic matrix composites. *Advances in Ceramic Matrix Composites*, 267–285.
- Xu, X., Lao, X., Wu, J., Zhang, Y., Xu, X., & Li, K. (2016). Synthesis and characterization of Al<sub>2</sub>O<sub>3</sub>/SiC composite ceramics via carbothermal reduction of aluminosilicate precursor for solar sensible thermal storage. *Journal of Alloys and Compounds*, 662, 126–137.
- Xu, X., Rao, Z., Wu, J., Li, Y., Zhang, Y., & Lao, X. (2014). Solar Energy Materials & Solar Cells In-situ synthesis and thermal shock resistance of cordierite / silicon carbide composites used for solar absorber coating. *Solar Energy Materials and Solar Cells*, 130, 257–263.
- Yang, H. J., Yuan, J., Li, Y., Hou, Z. L., Jin, H. B., Fang, X. Y., & Cao, M. S. (2013). Silicon carbide powders: Temperature-dependent dielectric properties and enhanced microwave absorption at gigahertz range. *Solid State Communications*, 163, 1–6.
- Ye, F., Zhang, L., Yin, X., Liu, Y., & Cheng, L. (2013). The improvement of wave-absorbing ability of silicon carbide fibers by depositing boron nitride coating. *Applied Surface Science*, 270, 611–616.
- Yi, J. W., Lee, S. B., Kim, J. B., Lee, S. K., & Park, O. O. (2014). Electromagnetic wave absorption properties of composites with ultrafine hollow magnetic fibers. *Journal of Magnetism and Magnetic Materials*, 361, 182–187.
- Yin, L., & Stoll, R. (2014). 26 - *Ceramics in restorative dentistry*. *Advances in Ceramic Matrix Composites* (Vol. 1). Woodhead Publishing Limited.
- Zhao, J. (2014). *The use of ceramic matrix composites for metal cutting applications*. *Advances in Ceramic Matrix Composites*. Woodhead Publishing Limited.

## APPENDIX

### Appendix A: Sponge under optical microscope

Sponge	Microstructure under Optical Microscope
<p data-bbox="531 450 560 483">A</p> 	 <p data-bbox="1070 1010 1385 1025">2000 μm</p>
<p data-bbox="531 1133 560 1167">B</p> 	

<p>C</p> 	
<p>D</p> 	
<p>E</p> 	

**Appendix B:** Pore Size for 5 different sponge

Sponge Type	Pore Size ( $\mu\text{m}$ )				
	Sponge A	Sponge B	Sponge C	Sponge D	Sponge E
1	249.4	361.6	394.6	855.9	466.8
2	505.5	448.8	762.5	486.8	490
3	384.4	362.5	377.6	756	708.8
4	341.9	507.8	644.7	628	773.9
5	399.4	459.3	532.9	548.1	680.2
6	292.5	367.4	516	617.2	658.5
7	285.3	372.5	889.7	1149	427.7
8	176.1	235.1	611.9	509.4	439.8
9	306.5	256.8	934	557.8	479.1
10	340	291.7	755.1	540.5	609.6
11	267.7	392.6	312	497	507.6
12	319	244.5	584.4	734.2	736.1
13	398.4	168.3	487.7	458.6	691.2
14	238.8	578.6	685.4	535.7	971.1
15	368.9	372.1	917.6	347.8	287.9
16	306.9	232.5	342.1	467.2	1451
17	365.5	304.2	680	449.9	658.2
18	353.5	173.9	725.2	272.9	521.8
19	190.9	160.1	602.2	476.4	311.8
20	272.4	201.7	274.9	570.4	482.6
21	170.2	123	255.7	379.5	552.7
22	217.6	264.2	576.7	301.6	666.8
23	308.4	276.2	568.1	276.4	854.1
24	370.6	397.4	535.7	739.9	674.2
25	297.3	182.5	498.7	642.3	421.2
26	465.6	422.2	652.7	557.9	357.3
27	311.1	477.8	204.2	890.4	311.8
28	7.233	282.7	506.7	524	399.4
29	262.1	329.9	424.3	167	752.9
30	289.4	499.4	381.9	745.6	258
N=	30	30	30	30	30
Mean=	302.0844	324.91	554.5067	556.1133	586.7367
STDv=	95.34645	117.6239	191.9523	204.0565	240.6092

KELANTAN



**Appendix C:** The density reading of sintered composite

Sample Code	Dry Weight (g)		Suspended (g)		Saturated(g)	
	Reading	Average	Reading	Average	Reading	Average
10 wt% Al <sub>2</sub> O <sub>3</sub>	0.11		0.066		0.118	
	0.109	0.1097	0.066	0.0667	0.115	0.1167
	0.111		0.068		0.117	
20 wt% Al <sub>2</sub> O <sub>3</sub>	0.101		0.068		0.126	
	0.1	0.0997	0.063	0.0647	0.123	0.124
	0.098		0.063		0.123	
30 wt% Al <sub>2</sub> O <sub>3</sub>	0.108		0.072		0.115	
	0.103	0.1063	0.07	0.071	0.116	0.1163
	0.108		0.071		0.118	
40 wt% Al <sub>2</sub> O <sub>3</sub>	0.104		0.068		0.127	
	0.102	0.1033	0.069	0.068	0.124	0.125
	0.104		0.067		0.124	
50 wt% Al <sub>2</sub> O <sub>3</sub>	0.108		0.074		0.131	
	0.111	0.11	0.07	0.072	0.121	0.1243
	0.111		0.072		0.121	

**Appendix D:** The bulk density and apparent density using formula

Sample Code	Bulk Density (g/cm <sup>3</sup> )	Apparent Porosity (%)
10 wt% Al <sub>2</sub> O <sub>3</sub>	2.194	714.2857
20 wt% Al <sub>2</sub> O <sub>3</sub>	1.6813	244.0329
30 wt% Al <sub>2</sub> O <sub>3</sub>	2.2466	453
40 wt% Al <sub>2</sub> O <sub>3</sub>	1.8123	262.6728
50 wt% Al <sub>2</sub> O <sub>3</sub>	2.1032	365.7343

UNIVERSITI  
MALAYSIA  
KELANTAN

**Appendix E:** Microwave absorption of sintered composited

Time (Minutes)	Temperature (°C)				
	10 wt% Al <sub>2</sub> O <sub>3</sub>	20 wt% Al <sub>2</sub> O <sub>3</sub>	30 wt% Al <sub>2</sub> O <sub>3</sub>	40 wt% Al <sub>2</sub> O <sub>3</sub>	50 wt% Al <sub>2</sub> O <sub>3</sub>
0.5	59	48	44	60	55
1	88	73	64	88	83
1.5	104	91	77	110	103
2	128	101	94	126	119
2.5	141	108	100	140	135
3	142	113	103	153	149
3.5	143	118	109	163	164
4	146	119	113	170	178
4.5	149	120	118	177	182
5	149	126	124	182	191
5.5	151	129	129	184	202
6	155	132	136	204	213
6.5	159	136	138	218	218
7	161	140	140	232	225
7.5	162	143	148	245	255
8	167	148	152	253	289
8.5	172	150	154	260	327
9	170	155	159	262	369
9.5	177	157	160	267	408
10	181	161	161	269	446
10.5	183	164	162	270	483
11	186	167	163	279	507
11.5	191	170	165	280	535
12	193	171	167	283	556

Appendix F: The pattern of COD 9009671

Pattern: COD 9009671 Radiation: 1.54060 Quality: Quality Unknown

Formula Al <sub>2</sub> O <sub>3</sub>			d	2θ	l	h	k	l
Name			3.48500	25.539	616	-1	1	-2
Name (mineral) Corundum			2.55460	35.100	943	-1	1	4
Name (common)			2.38280	37.722	440	-2	1	0
			2.16830	41.618	4	0	0	-6
			2.08840	43.289	982	-2	1	-3
			1.96700	46.110	15	-2	2	2
			1.74250	52.472	495	-2	2	-4
Lattice: Hexagonal			1.60370	57.413	999	-2	1	-6
S.G.: R-3c (167)			1.54880	59.650	26	-3	1	-1
Mol. weight =			1.51690	61.036	33	-3	1	2
Volume [CD] = 255.89			1.51300	61.211	73	-1	1	-8
Dx =			1.40650	66.415	395	-3	1	-4
Dm =			1.37570	68.102	611	-3	0	0
V <sub>cor</sub> = 1.110			1.33790	70.305	13	-3	1	5
a = 4.76570	alpha =		1.27730	74.180	14	-2	2	8
b =	beta =		1.24080	76.750	179	-1	1	10
c = 13.01000	gamma =		1.23590	77.111	95	-2	1	-9
a/b = 1.00000	Z =		1.19490	80.280	8	-3	1	-7
c/b = 2.72992			1.19140	80.564	70	-4	2	0
			1.16170	83.070	4	-3	0	-6
			1.16170	83.070	4	-3	0	6
			1.14890	84.206	57	-4	2	-3
			1.14030	84.990	3	-4	1	1
			1.12740	86.197	43	-4	1	-2
			1.12580	86.349	29	-3	1	8
			1.10050	88.847	85	-2	2	-10
			1.08420	90.548	21	0	0	-12
			1.07980	91.020	100	-4	1	4
			1.04780	94.641	2	-4	1	-5
			1.04420	95.071	206	-4	2	-6
			1.01910	98.202	28	-4	4	-2
Primary Reference								
dAmour H, Schiferl D., Denner W., Schulz H., Holzappel W. B., "High-pressure single-crystal structure determinations for ruby up to 90 kbar using an automatic diffractometer P = 0 kbar", Journal of Applied Physics 49 (1978) 4411-4416.								
Radiation: Wavelength: 1.54060			Filter: Not specified					
SS/FOM:			d-spacing:					

Appendix G: The pattern of COD 1011053

Pattern: COD 1011053 Radiation: 1.54060 Quality: Quality Unknown

Formula		Si C		d	2 $\theta$	l	h	k	l
Name				2.63950	33.936	562	-1	0	-1
Name (mineral)		Moissanite 6H		2.52830	35.477	667	0	0	-6
Name (common)				2.52720	35.493	999	-1	0	-2
				2.36820	37.964	590	-1	0	-3
				2.18890	41.209	234	-1	0	-4
				2.00870	45.099	88	-1	0	-5
				1.68520	54.400	112	-1	0	-7
Lattice:		Hexagonal		1.54800	59.684	271	-1	0	-8
S.G.:		P 63 (173)		1.54750	59.705	539	-2	1	0
		Mol. weight =		1.42690	65.346	234	-1	0	-9
		Volume [CD] = 125.85		1.33500	70.480	45	-2	0	-1
		Dx =		1.32020	71.390	94	-1	0	-10
		Dm =		1.31990	71.409	378	-2	1	-6
		V/cor = 1.420		1.31970	71.421	95	-2	0	-2
a = 3.09500	alpha =			1.29540	72.974	75	-2	0	-3
b =	beta =			1.26420	75.080	26	0	0	-12
c = 15.17000	gamma =			1.26360	75.122	39	-2	0	-4
a/b = 1.00000	Z = 6			1.22630	77.827	15	-1	0	-11
c/b = 4.90145				1.22590	77.858	15	-2	0	-5
				1.13980	85.036	24	-2	0	-7
				1.09440	89.474	71	-2	0	-8
				1.06990	92.105	9	-1	0	-13
				1.04900	94.499	76	-2	0	-9
				1.01080	99.294	17	-3	1	-1
				1.01080	99.294	17	-3	2	-1
Primary Reference		Ott H, "Die Gitterstruktur des Karborunds ( Si C ) I.", Zeitschrift fuer Kristallographie, Kristallgeometrie, Kristallphysik, Kristallchemie (-144,1977) 61 (1925) 515-531.							
Radiation:		Filter:	Not specified						
Wavelength	1.54060	d-spacing:							
h:									
SS/FOM:									

Appendix H: Microwave absorption of sintered composited

Time (Minutes)	Temperature				
	Sponge A	Sponge B	Sponge C	Sponge D	Sponge E
0.5	60	62	60	55	70
1	101	74	83	93	95
1.5	120	98	117	115	117
2	130	104	136	145	128
2.5	155	112	152	152	135
3	172	129	173	164	162
3.5	187	141	201	173	196
4	193	153	218	182	206
4.5	205	163	235	204	237
5	237	184	256	218	242
5.5	246	195	273	284	274
6	253	228	288	316	295
6.5	261	245	309	325	308
7	268	257	334	332	316
7.5	270	273	351	351	325
8	273	295	387	360	332
8.5	281	318	406	367	345
9	285	338	437	372	406
9.5	292	369	463	381	416
10	302	411	491	390	452
10.5	304	439	512	417	481
11	311	450	531	419	493
11.5	317	472	557	425	509
12	322	483	591	436	525